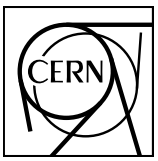
arXiv:1208.5717v2 [hep-ex] 1 Oct 2012

EUROPEAN ORGANIZATION FOR NUCLEAR RESEARCH





CERN-PH-EP-2012-221
October 2, 2012

Production of $K^*(892)^0$ and $\phi(1020)$ in pp collisions at $\sqrt{s}$=7 TeV

The ALICE Collaboration*

Abstract

The production of $K^*(892)^0$ and $\phi(1020)$ in pp collisions at $\sqrt{s}$=7 TeV was measured by the ALICE experiment at the LHC. The yields and the transverse momentum spectra $d^2N/dyd p_T$ at midrapidity $|y|< 0.5$ in the range $0<p_T<6$ GeV/c for $K^*(892)^0$ and $0.4<p_T<6$ GeV/c for $\phi(1020)$ are reported and compared to model predictions. Using the yield of pions, kaons, and Ω baryons measured previously by ALICE at $\sqrt{s}$=7 TeV, the ratios K^*/K^-, ϕ/K^*, ϕ/K^-, ϕ/π^-, and $(\Omega+\overline{\Omega})/\phi$ are presented. The values of the K^*/K^-, ϕ/K^* and ϕ/K^- ratios are similar to those found at lower centre-of-mass energies. In contrast, the ϕ/π^- ratio, which has been observed to increase with energy, seems to saturate above 200 GeV. The $(\Omega+\overline{\Omega})/\phi$ ratio in the p_T range 1-5 GeV/c is found to be in good agreement with the prediction of the HIJING/B$\overline{\text{B}}$ v2.0 model with a strong colour field.

*See Appendix A for the list of collaboration members

1 Introduction

The study of resonance production plays an important role in both elementary and heavy ion collisions. In pp and e^+e^- collisions it contributes to the understanding of hadron production [1, 2] as the decay products of resonances represent a large fraction of the final state particles. In addition, it provides a reference for tuning event generators inspired by Quantum Chromodynamics (QCD). In heavy ion collisions, resonances are a sensitive probe of the dynamical evolution of the fireball. Due to their short lifetime (a few fm/c) a significant fraction of resonances decay inside the hot and dense medium and their hadronic daughters interact with the medium during the fireball expansion [3, 4, 5].

The $\phi(1020)$, which is the lightest vector meson composed only of sea quarks, provides a probe for the study of the strangeness production. In pp collisions, $s\bar{s}$ pair production was found to be significantly suppressed in comparison to $u\bar{u}$ and $d\bar{d}$-pair [6, 7]. Another useful probe of strangeness production is the $K^*(892)^0$, which is a vector meson with a mass similar to the ϕ, but differing by one unit of the strangeness quantum number. The $(\Omega+\overline{\Omega})/\phi$ ratio has been suggested [8] as a probe of the colour field strength, which in microscopic models influences the relative yield of strange with respect to non-strange particles.

We present the first measurement of the differential ($\mathrm{d}^2N/\mathrm{d}y\mathrm{d}p_\mathrm{T}$) and p_T-integrated ($\mathrm{d}N/\mathrm{d}y$) yields of the K^* [1] and $\phi(1020)$ mesons at midrapidity ($|y|<0.5$) in pp collisions at $\sqrt{s}$=7 TeV. The data analysis was carried out for K^* (ϕ) on a sample of 80 (60) million minimum bias pp collisions collected by the ALICE experiment. The resonances were identified via their main decay channel $K^* \longrightarrow \pi^{\pm}$+$K^{\mp}$ and $\phi \longrightarrow K^+$+K^-. Tracks were reconstructed by the main ALICE tracking devices, the Time Projection Chamber (TPC) and the Inner Tracking System (ITS). The TPC and Time of Flight (TOF) detectors were used to identify pions and kaons. The measured spectra are compared to two QCD-based event generators, PHOJET [9] and PYTHIA [10].

The ratios K^*/K^-, ϕ/K^*, ϕ/K^-, and ϕ/π^- are computed using the yield of pions and kaons measured [11] with the ALICE detector in pp collisions at 7 TeV. These ratios are compared with measurements at lower collision energies. The $(\Omega+\overline{\Omega})/\phi$ ratio has been calculated as a function of transverse momentum using the Ω and $\overline{\Omega}$ yield measured at 7 TeV [12]; this ratio is then compared to the predictions of the HIJING/B$\overline{\mathrm{B}}$ v2.0 model with a Strong Colour Field (SCF) [13] and to PYTHIA-Perugia 2011 [14].

The article is organized as follows: Section 2 gives details about the detectors relevant for this analysis, Section 3 describes the criteria used for event selection, Section 4 gives an overview of the analysis, Section 5 presents the results and Section 6 the conclusions.

2 Experimental set-up

A full description of the ALICE detector can be found in [15, 16]. For the analyses described in this paper, the ITS, the TPC, and the TOF detectors were used. These detectors are set inside a large solenoidal magnet providing a magnetic field B=0.5 T, and have a common pseudorapidity coverage of $|\eta| < 0.9$. Two forward scintillator hodoscopes (VZERO) placed along the beam direction at -0.9 m and 3.3 m on either side of the interaction point, cover the pseudorapidity regions $-3.7 < \eta < -1.7$ and $2.8 < \eta < 5.1$. These are used for triggering and for rejecting beam-gas interactions.

2.1 The Inner Tracking System

The ITS [16] is the innermost ALICE detector, located between 3.9 and 43 cm radial distance from the beam axis. It is made of six cylindrical layers of silicon detectors (two layers of pixels, two of silicon drift, and two of silicon strips), with a total material budget of 7.66 % of the radiation length X_0. It

[1] We denote by K^* the average of $K^*(892)^0$ and $\overline{K^*(892)^0}$.

provides high-resolution space points close to the interaction vertex, thus improving momentum and angular resolution of the tracks reconstructed in the TPC.

The two innermost ITS layers constitute the Silicon Pixel Detector (SPD), which has a high granularity of about 9.8 million pixel cells, each with a size of 50×425 μm^2. These layers are located at radii of 3.9 and 7.6 cm with pseudorapidity coverages of $|\eta| < 2.0$ and $|\eta| < 1.4$, respectively. The detector provides a position resolution of 12 μm in the $r\varphi$ direction and about 100 μm in the direction along the beam axis.

2.2 The Time Projection Chamber

The TPC [17] is the main ALICE tracking device. It is a large-volume, high-granularity, cylindrical drift detector which has a length of 5.1 m and inner and outer radii of 0.85 and 2.47 m, respectively. It covers the pseudorapidity range $|\eta| < 0.9$ with a full azimuthal acceptance. The drift volume is filled with 90 m^3 of $Ne/CO_2/N_2$. The maximum drift time is 94 μs. A total of 72 multi-wire proportional chambers with cathode pad readout instrument the two end plates, which are segmented into 18 sectors and include a total of over 550,000 readout pads. The ionization electrons drift for up to 2.5 m and are measured on 159 pad rows. The momentum resolution of the TPC is in the range 1-7% for pions with $1<p_{\rm T}<10$ GeV/c. The ALICE TPC ReadOut (ALTRO) chip, employing a 10 bit ADC at 10 MHz sampling rate and digital filtering circuits, allows for precise position and linear energy loss measurements with a gas gain of the order of 10^4. The material budget of the TPC near $\eta = 0$ amounts to about 4.1% of X_0.

The position resolution in the $r\varphi$ direction varies between 1100 μm and 800 μm going from the inner to the outer radius, whereas the resolution along the beam axis varies between 1250 μm and 1100 μm.

2.3 The Time Of Flight detector

The ALICE TOF [18, 19] is a cylindrical assembly of Multi-gap Resistive Plate Chambers (MRPC) with an inner radius of 370 cm and an outer radius of 399 cm. It has a pseudorapidity coverage of $|\eta| < 0.9$ and full azimuthal acceptance, except for the region $260^{\rm o} < \varphi < 320^{\rm o}$ at $|\eta| < 0.14$ where a gap was left in order to reduce the amount of material in front of the Photon Spectrometer (PHOS). The elementary unit of the TOF system is a 10-gap double-stack MRPC strip 122 cm long and 13 cm wide, with an active area of 120×7.4 cm^2 subdivided into two rows of 48 pads of 3.5×2.5 cm^2 each. The length of the TOF barrel active region is 741 cm. It has about 153,000 readout channels and an average thickness of 25-30% of X_0, depending on the detector zone. For pp collisions, such a segmentation leads to an occupancy below 0.02%. The front-end electronics are designed to comply with the basic characteristics of the MRPC detector, i.e. very fast differential signals from the anode and the cathode readout: the resulting intrinsic time resolution of the detector and electronics was measured to be smaller than 50 ps.

3 Data collection and event selection

Data used for this analysis were collected in 2010 using a magnetic field of B=0.5 T with both field polarities. The minimum bias trigger required a single hit in the SPD detector or in one of the two VZERO counters, i.e. at least one charged particle anywhere in the $\sim$8 units of pseudorapidity covered by these detectors. In addition, a coincidence was required with signals from two beam pick-up counters, one on each side of the interaction region, indicating the passage of proton bunches. The trigger selection efficiency for inelastic collisions was estimated to be 85.2% with a +6.2% and -3% relative uncertainty [20]. During the data-taking period, the luminosity at the ALICE interaction point was kept in the range $0.6-1.2\times10^{29}$ cm^{-2}s^{-1}. Runs with a mean pile-up probability per event larger than 5% were excluded from the analysis.

Beam-induced background was reduced to a negligible level (< 0.01%) with the help of the timing information of the VZERO counters and by a cut on the position of the primary vertex reconstructed

by the SPD [21]. Accepted events were required to have a reconstructed primary vertex. Its position can be computed either using the tracks reconstructed by TPC and ITS, or using the "tracklets" obtained connecting reconstructed clusters in both SPD layers. If possible, the first method is used. First, for each event a three dimensional reconstruction of the primary vertex was attempted with either a Kalman filter, using reconstructed tracks as input, or by a minimization of the squared distances between all the extrapolated tracklets. Otherwise only the z position of the primary vertex was reconstructed by correlating the z coordinates of the SPD space points, while for x and y the average position of the beam in the transverse plane was taken. The primary vertex reconstrunction efficiency, calculated via Monte Carlo simulation, approaches unity in events with a K^* or a ϕ produced in the central rapidity region. In order to minimize acceptance and efficiency biases for tracks at the edge of the TPC detection volume, events were accepted only when their primary vertex was within $\pm$10 cm from the geometrical centre of the ALICE barrel.

4 Data analysis

4.1 Track selection

Global tracking in ALICE is performed using ITS and TPC clusters. It is based on a Kalman filter algorithm which takes into account both multiple scattering and energy loss along the path as described in detail in [22]. The Distance of Closest Approach (DCA) to the primary vertex is used to discriminate between primary and secondary particles. Primary charged particles are those produced directly in the interaction and all decay products from particles with a proper decay length $c\tau$ <1 cm; secondary particles include those from the weak decay of strange hadrons and from interactions in the detector material. Several cuts were applied to achieve a high track quality in the analyzed sample. Tracks were required to have at least 70 reconstructed clusters in the TPC out of the maximum 159 available. This ensured a high efficiency and good dE/dx resolution, keeping the contamination from secondary and fake tracks small.

In order to improve the global resolution, tracks were accepted only in the range $|\eta| < 0.8$ (i.e. well within the TPC acceptance) and with $p_{\rm T}>$ 0.15 GeV/c. In order to reduce secondary particles, tracks were required to have at least one hit in one of the two innermost tracking detectors (SPD) and to have a DCA to the primary vertex less than 2 cm along the beam direction. The DCA in the transverse plane was required to be smaller than 7 $\sigma_{\rm DCA}(p_{\rm T})$, where $\sigma_{\rm DCA}(p_{\rm T})$ = (0.0026 + 0.0050 GeV/c $\cdot p_{\rm T}{}^{-1}$) cm.

4.2 Particle identification

Identification of pions and kaons is performed using the measurements of the TPC and the TOF. For the TPC, the particle is identified based on the energy it deposits in the drift gas, compared with the expected value computed using a parameterized Bethe-Bloch function [23, 24]. Figure 1 shows the TPC signal versus track momentum computed at the point the particle enters the detector, and the curves represent the Bethe-Bloch functions for each mass hypothesis. The TPC calibration parameters have mostly been determined and tested via the analysis of cosmic rays; the chamber gain has been measured using the decay of radioactive ^{83}Kr gas released into the TPC volume [17].

A truncated-mean procedure is used to determine dE/dx, with only 60% of the points kept. The dE/dx resolution $\sigma_{\rm TPC}$ is about 5% for tracks with 159 clusters and about 6.5% when averaged over all reconstructed tracks. The relevant value of $\sigma_{\rm TPC}$ is estimated for each track taking into account the actual number of clusters used [17].

The TPC dE/dx measurement allows pions to be separated from kaons for momenta up to $p \sim 0.7$ GeV/c, while the proton/antiproton band starts to overlap with the pion/kaon band at $p \approx$1 GeV/c. As can be observed in Fig. 1, the electron/positron dE/dx band crosses the other bands at various momenta. This contamination in identified pions and kaons can be drastically reduced using information from the TOF.

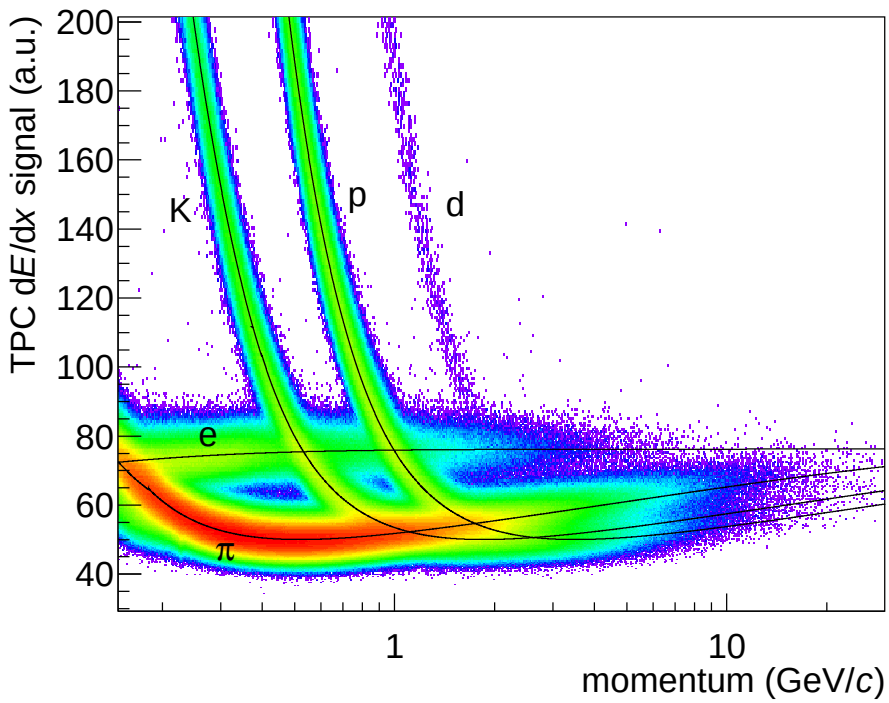


Fig. 1: (Colour online) Specific ionization energy loss dE/dx vs. momentum for tracks measured with the ALICE TPC. The solid lines are parametrizations of the Bethe-Bloch function [23].

Particles are identified in the TPC via the difference between the measured energy loss and the value expected for different mass hypotheses. The cut on this difference, normalized to the resolution σ_{TPC}, is optimized for each analysis and depends in general on the signal-to-background ratio and on the transverse momentum.

Figure 2 shows the correlation between particle momentum and their velocity $\beta = L/ct$, where L is the total integrated path length and t is the time of flight measured by the TOF detector. For the analyses described in this paper the start time of the collision is estimated using the particle arrival times at the TOF or the averaged collision time observed in the fill. The bands corresponding to pions, kaons, protons and deuterons are clearly visible.

Particles are identified in the TOF by comparing the measured time of flight to the expected time for a given particle species. The cut is expressed in units of the estimated resolution σ_{TOF} for each track, which has a mean value of 160 ps. The TOF allows pions and kaons to be unambigously identifed up to $p \sim 1.5$ GeV/c. The two mesons can be distinguished from (anti)protons up to $p \sim 2.5$ GeV/c.

Considering the high multiplicities reached in pp collisions at LHC energies, good particle identification is important to reduce combinatorial background as well as correlated background from misidentified resonance decays. The ϕ analysis requires only primary kaons to be selected and cuts were kept loose in order to maximize the efficiency. The cut for particle identification in the TPC was set to $3\sigma_{\mathrm{TPC}}$ ($5\sigma_{\mathrm{TPC}}$) for tracks with p larger (smaller) than 0.35 GeV/c. When a TOF signal is present, a particle identification cut of $3\sigma_{\mathrm{TOF}}$ is also applied. For the K* analysis, both pions and kaons are identified. Two different strategies were followed. For tracks with TOF signals, a TPC dE/dx cut of $5\sigma_{\mathrm{TPC}}$ was applied and a TOF cut of $3\sigma_{\mathrm{TOF}}$ ($2\sigma_{\mathrm{TOF}}$) was applied for tracks with momenta below (above) 1.5 GeV/c. For tracks without a TOF signal the kaon momentum was required to be below 0.7 GeV/cand $5\sigma_{\mathrm{TPC}}$, $3\sigma_{\mathrm{TPC}}$, and $2\sigma_{\mathrm{TPC}}$ cuts were used for $p <$0.35 GeV/c, 0.35$< p <$ 0.5 GeV/c, and $p >$ 0.5 GeV/c, respectively. This more restrictive cut on kaons was used to reduce the correlated background originating from ρ

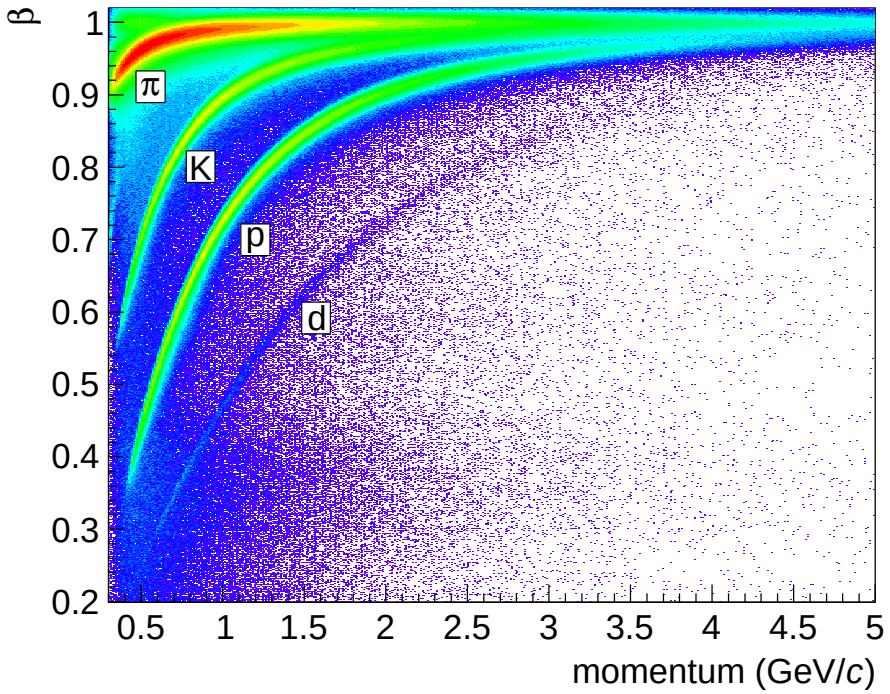


Fig. 2: (Colour online) Velocity β of particles measured by TOF vs. momentum.

decays in which a pion is misindentified.

4.3 Raw yield extraction and background estimation

The uncorrelated background was estimated using two different techniques: like-sign and event mixing. In the like-sign method invariant mass distributions of like-sign Kπ or KK combinations (for K* and ϕ, respectively) from the same event were constructed. In the event mixing method the shape of the uncorrelated background was estimated from the invariant mass distribution of unlike-sign Kπ or KK combinations from different events. To avoid mismatch due to different acceptances and to assure a similar event structure, tracks from events with similar vertex positions z ($\Delta z < 1$ cm) and track multiplicities n ($\Delta n < 10$) were mixed. To reduce statistical uncertainties each event was mixed with 10 other events. The mixed-event distribution was then normalized in the mass region $1.08 < M < 1.2$ ($1.04 < M < 1.07$) GeV/c^2 for K* (ϕ), and subtracted in each $p_{\rm T}$ bin. The uncertainty in the normalization was estimated by varying the normalization region and is included in the quoted systematic uncertainty for signal extraction. After background subtraction a residual background remains. This is due in part to an imperfect description of the combinatorial background but mainly caused by a real correlated background. The latter can arise from correlated πK or KK pairs or from misidentified particle decays (for example K^{*0} for ϕ, or ϕ and ρ for K*, or from underlying jet event structure).

The total $p_{\rm T}$-integrated number of reconstructed mesons after background subtraction was about 1.8×10^6 for the K* and 2.3×10^5 for the ϕ. For the K* the signal-to-background ratio varied from 0.08 at $p_{\rm T}$=0.05 GeV/c to 0.2 at $p_{\rm T}$= 5.5 GeV/c. The significance ($S/\sqrt{S+B}$) was about 34 in the $p_{\rm T}$ bins at both 0.05 and 5.5 GeV/c and reached a maximum of about 127 at 1 GeV/c. For the ϕ the signal-to-background ratio varied from 2.8 to 1.6 between $p_{\rm T}$=0.45 and $p_{\rm T}$=5.5 GeV/c, with a minimum of 0.5 at 1.6 GeV/c; the significance was about 30 in the $p_{\rm T}$ bins at both 0.45 and 5.5 GeV/c with a maximum of 90 at 1 GeV/c.

The raw yield of K*(892)^0 and its antiparticle was extracted in 22 $p_{\rm T}$ bins between 0 and 6 GeV/c in the rapidity range $|y|< 0.5$. The combinatorial background was subtracted using like-sign $\pi^{\pm}$K$^{\pm}$ pairs.

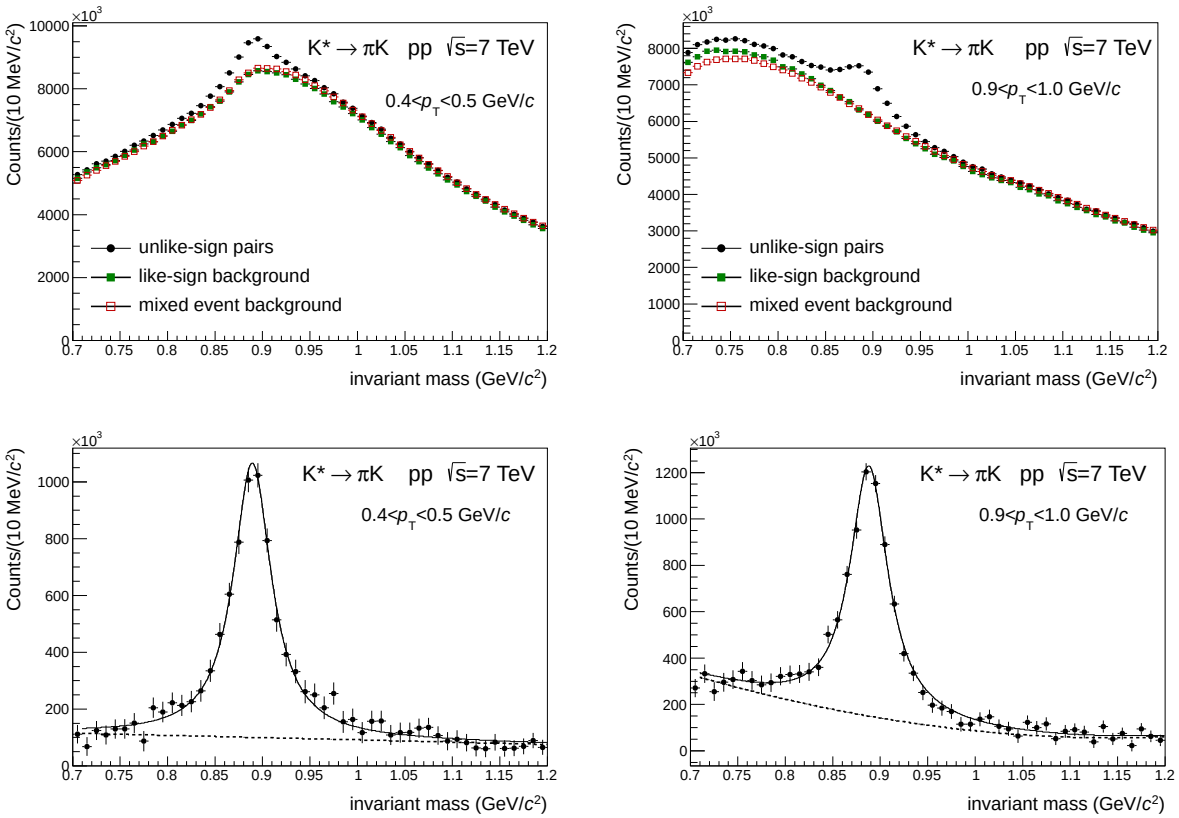


Fig. 3: (Colour online) (Upper panel) The $\pi^{\pm}K^{\mp}$ invariant mass distribution in $|y|<0.5$ for the bin $0.4<p_{\mathrm{T}}<0.5$ GeV/c (left) and $0.9<p_{\mathrm{T}}<1.0$ GeV/c (right), in pp collisions at 7 TeV. The background shape estimated using unlike-sign pairs from different events (event mixing) and like-sign pairs from the same event are shown as open red squares and full green squares, respectively. (Lower panel) The $\pi^{\pm}K^{\mp}$ invariant mass distribution after like-sign background subtraction for $0.4<p_{\mathrm{T}}<0.5$ GeV/c (left) and $0.9<p_{\mathrm{T}}<1.0$ GeV/c (right). The solid curve is the result of the fit by Eq. 1, the dashed line describes the residual background.

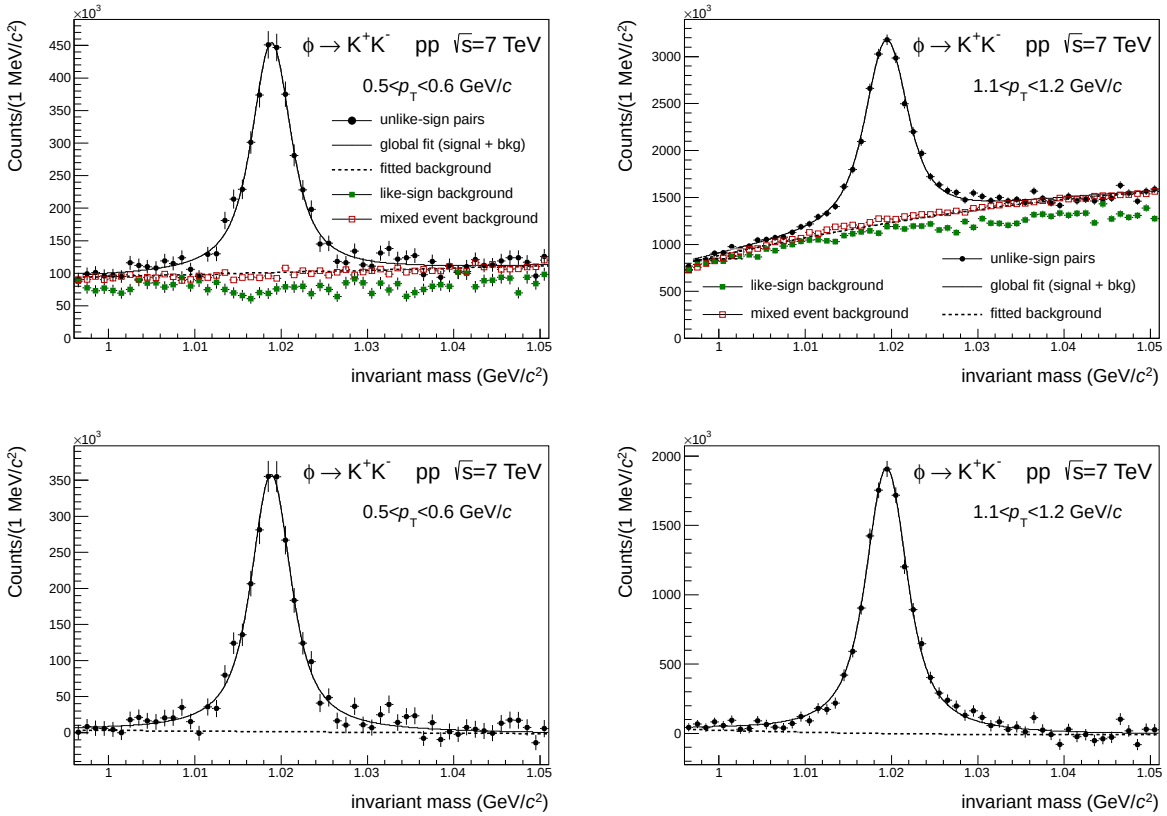


Fig. 4: (Colour online) (Upper panel) The K^+K^- invariant mass distribution in $|y|<0.5$, for the bin $0.5<p_T<0.6$ GeV/c (left) and $1.1<p_T<1.2$ GeV/c (right) in pp collisions at 7 TeV. The solid curve is the fit result (Eq. 2), while the dashed line describes the background. The background shape estimated using unlike-sign pairs from different events (event mixing) or like-sign pairs from the same event are shown as open red squares and full green squares, respectively. (Lower panel) The K^+K^- invariant mass distribution after mixed-event background subtraction for $0.5<p_T<0.6$ GeV/c (left) and $1.1<p_T<1.2$ GeV/c (right). The solid curve is the fit result (Eq. 2), while the dashed line describes the residual background.

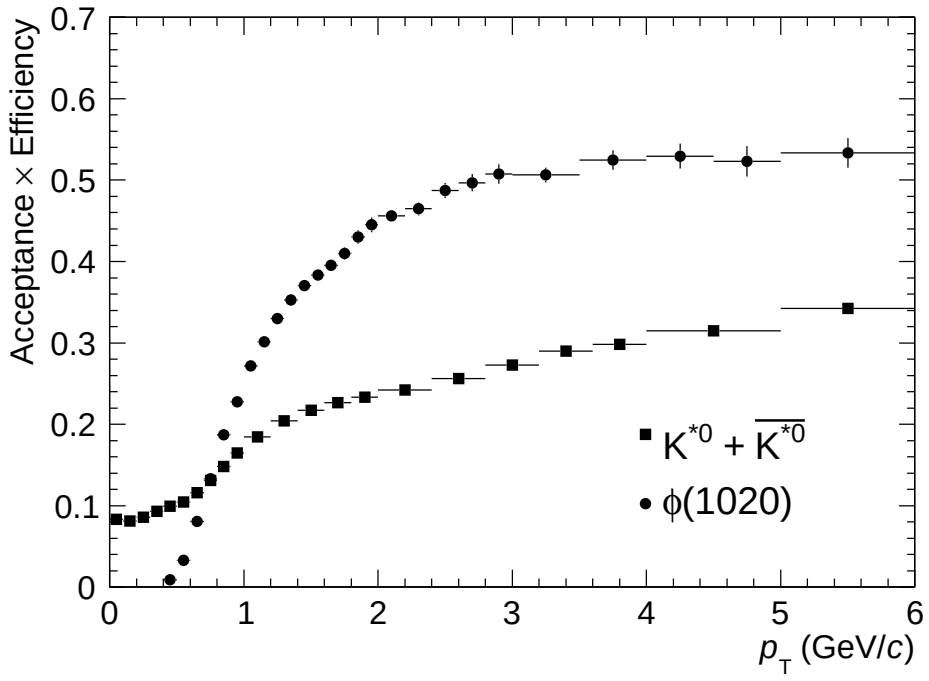


Fig. 5: The product of acceptance and efficiency of K^* and ϕ detection as a function of p_T in $|y|<0.5$. Statistical uncertainties are reported. Contributions to the point-to-point systematic uncertainties are listed in Tab. 1.

The mass distribution $M(\pi^{\pm},K^{\mp})$ (see Fig. 3 for two p_T bins) was fitted with a relativistic Breit-Wigner function multiplied by a Boltzmann factor [3] and added to a polynomial residual background. The width was found to be compatible, within uncertainties, with the natural value. At low p_T the fitted mass values were found to be slightly lower (by about $\approx$5 MeV/c^2) than the natural value, which is attributed to imperfections in corrections for the energy loss in the detector material. To extract the yield the distribution of $M(\pi^{\pm},K^{\mp})$ was then fitted with a (non-relativistic) Breit-Wigner function with the width fixed to its natural value (Γ= 48.7 $\pm$0.8 [25]) and a background function:

$$\frac{\mathrm{d}N}{\mathrm{d}M} = \frac{1}{2\pi}\frac{A\Gamma}{(M-M_0)^2+\Gamma^2/4} + B(M) \tag{1}$$

where A is the area under the peak corresponding to the number of K^* mesons, Γ is the full width at half maximum of the peak, and M_0 is the resonance mass. The residual background $B(M)$, after like-sign subtraction, was parametrized by a polynomial (dashed line in Fig. 3).

For the ϕ meson, the raw yield was extracted from the K^+K^- invariant mass distributions in 26 p_T bins between 0.4 and 6 GeV/c. The combinatorial background was subtracted using a polynomial fit (first or second order), like-sign pairs, or unlike-sign pairs from mixed events (Fig. 4 for two p_T bins). Since the invariant mass resolution of the ϕ peak is of the same order of magnitude as the natural ϕ width ($\sim$1 MeV/c^2 vs. 4.26 MeV/c^2), the fit is performed, after background subtraction, using a Voigtian function (convolution of Breit-Wigner function and Gaussian) superimposed on a polynomial to describe the residual background:

$$\frac{\mathrm{d}N}{\mathrm{d}M} = A\int \frac{\Gamma/2\pi}{(M-M')^2+\Gamma^2/4}\frac{e^{-(M'-M_0)^2/2\sigma^2}}{\sqrt{2\pi}\sigma}\mathrm{d}M' + B(M) \tag{2}$$

where σ represents the mass resolution and the other parameters have the same meaning as in Eq. (1).

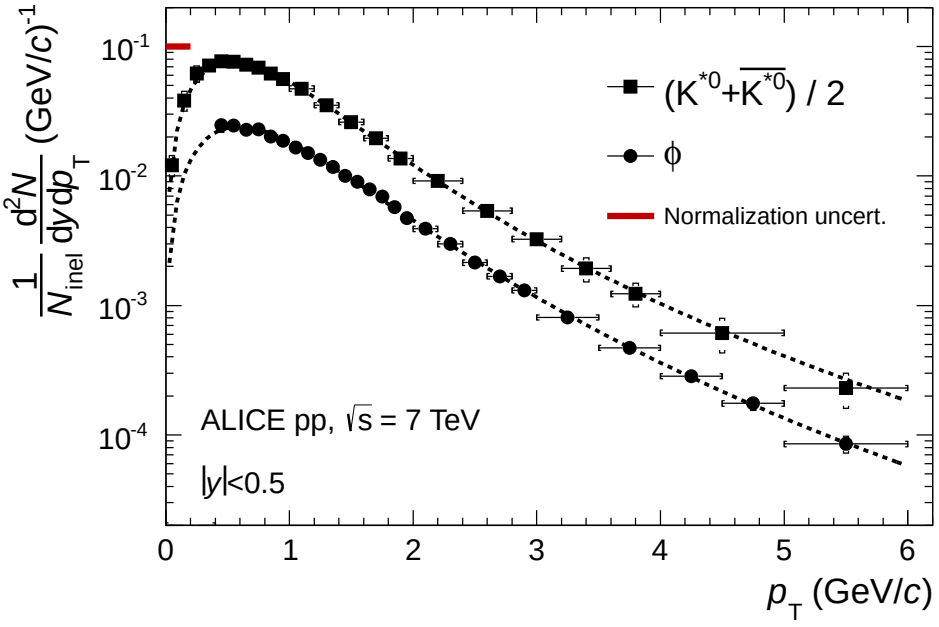


Fig. 6: Transverse momentum spectra for K* and ϕ(1020) in pp collisions at $\sqrt{s}$=7 TeV. The statistical and systematic uncertainties are added in quadrature and the uncertainty due to normalization [20] is shown separately. The statistical uncertainty is smaller than the symbol size. Each spectrum is fitted with a Lévy-Tsallis function (dashed line).

The background $B(M)$ is represented in the lower panels of Fig. 4 by a dashed line. The width Γ is fixed to its nominal value [25] while σ is a free parameter. The fitted mass values were found to be compatible, within uncertainties, with the known mass [25], with the exception of the low $p_{\rm T}$ range 0.4-0.7 GeV/c where a fitted value lower than the natural one (by $< 0.1\%$) was observed. The raw yields extracted using the three different methods to estimate the combinatorial background (analytic function, like-sign and mixed-event method) were found to be compatible within a few percent; therefore the mean value of all three methods was taken in each $p_{\rm T}$ bin.

4.4 Efficiency corrections

In order to extract the meson yields, the raw counts ($N^{\rm RAW}$) were corrected for the decay branching ratio [25] and for losses due to pion/kaon in-flight decays, geometrical acceptance, and detector efficiency ($N^{\rm cor} = N^{\rm RAW}/(A \times \varepsilon)$BR, where BR indicates the decay branching ratio). The product of acceptance and efficiency ($A \times \varepsilon$) was determined for K* and ϕ from Monte Carlo simulations with the PYTHIA 6.4 event generator (tune Perugia 0 [14]) and a GEANT3-based simulation of the ALICE detector response. About 60 M Monte Carlo events, with the same vertex distribution as the measured events, were analyzed in exactly the same way as the data. The dependence on the event generator was estimated to be below 1% by comparing PYTHIA and PHOJET simulated events. The $A \times \varepsilon$ was determined from the Monte Carlo simulations as the ratio of the number of reconstructed resonances to the number of those generated, differentially as a function of rapidity and transverse momentum. The transverse momentum dependence is shown in Fig. 5 for K* and ϕ mesons. The decrease in $A \times \varepsilon$ at low $p_{\rm T}$ is due to the minimum $p_{\rm T}$ requirement for reconstructed tracks, while the different behaviour for ϕ and K* is due to the different Q-value of their decay (31.1 MeV for ϕ and 262.7 MeV for K*).

Finally, corrections for the trigger efficiency ($\varepsilon_{\rm trigger}$) and the required primary vertex range ($\varepsilon_{\rm vert}$) were applied in order to obtain the absolute resonance yields per inelastic collision:

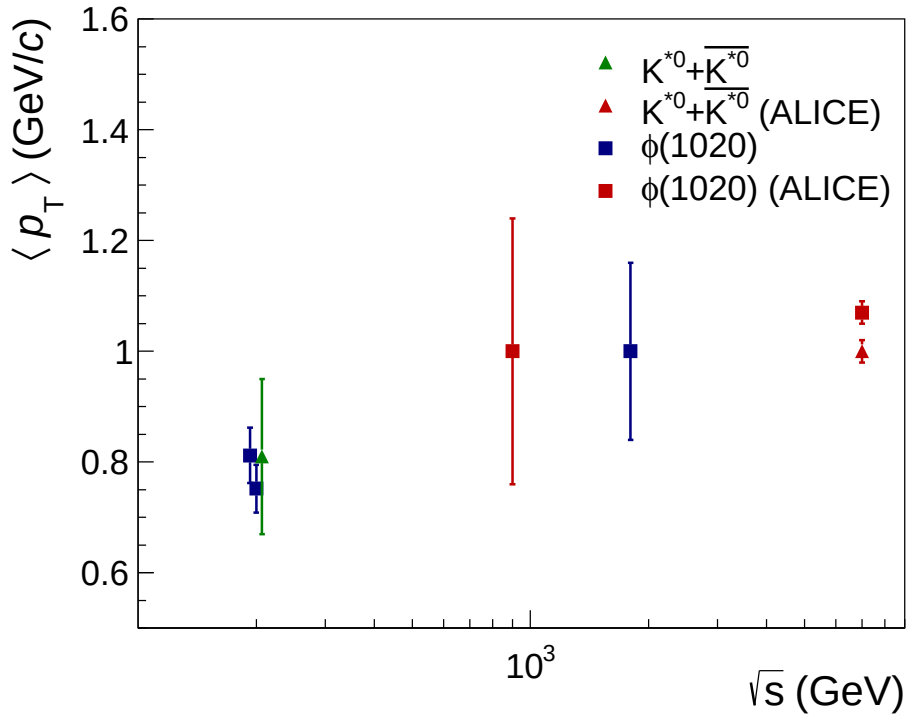


Fig. 7: Energy dependence of $\langle p_T \rangle$ for K* (triangles) and ϕ (squares) in pp collisions. The points at lower energies are from STAR and PHENIX ($\sqrt{s}$=200 GeV) [3, 5, 28], ALICE ($\sqrt{s}$=0.9 TeV) [32] and E735 ($\sqrt{s}$=1.8 TeV) [33]. The STAR data have been slightly displaced to separate the K* and the ϕ. The data point at 1.8 TeV represents the mean of the two values quoted from the E735 collaboration in [33], obtained from two different fit functions of the ϕ p_T distribution.

$$\frac{d^2N}{dydp_T} = \frac{N^{cor}(p_T)}{\Delta y \Delta p_T} \times \frac{1}{\varepsilon_{vert}} \times \frac{\varepsilon_{trigger}}{N_{MB}} \tag{3}$$

here N^{cor} and N_{MB} are the number of reconstructed K* or ϕ and the total number of minimum bias triggers, respectively. The value of the trigger selection efficiency for inelastic collisions $\varepsilon_{trigger}$ is reported in Section 3. The loss of resonances due to the trigger selection, estimated by Monte Carlo, is negligible, less than 0.2%. The ε_{vert} correction factor accounts for resonance losses (≈1%) due to the requirement to have a vertex in the range of ±10 cm.

4.5 Estimation of the systematic uncertainties

The minimum and maximum values of the major contributions to the point-to-point systematic uncertainties are listed in Tab. 1. The uncertainty due to the raw yield extraction method was found to be ±2-28% (2-10%) for K* (ϕ). It was estimated by changing the mass range considered for the fit and the order of the polynomial for the residual background function (from first through third (second) order for K* (ϕ)). Finally, variations in the yield due to the method used to estimate the combinatorial background (like-sign and event-mixing method and also analytic function for ϕ) were incorporated into the systematic uncertainties. For the K* a relativistic Breit-Wigner function was used to fit the mass peak in addition to the non-relativistic version. In the case of the K* a rather large systematic uncertainty was estimated for the higher p_T bins, due to the presence of a correlated background.

The uncertainty introduced by the tracking and PID efficiency was estimated to be ±8% (8%) and ±1-6% (1.5%) respectively in the case of K* (ϕ) by varying the kinematical and PID cuts on the daughter tracks. An additional ±1-4% uncertainty was added for the K* due to differences observed in the TOF matching

Table 1: Summary of the systematic point-to-point uncertainties in the K* and ϕ yield

Source of uncertainty	K*	ϕ
Signal extraction	$\pm$ 2-28 %	$\pm$ 2-10%
Tracking efficiency	$\pm$ 8 %	$\pm$ 8 %
PID efficiency	$\pm$ 1-6 %	$\pm$ 1.5 %
TOF matching efficiency	$\pm$ 1-4 %	-

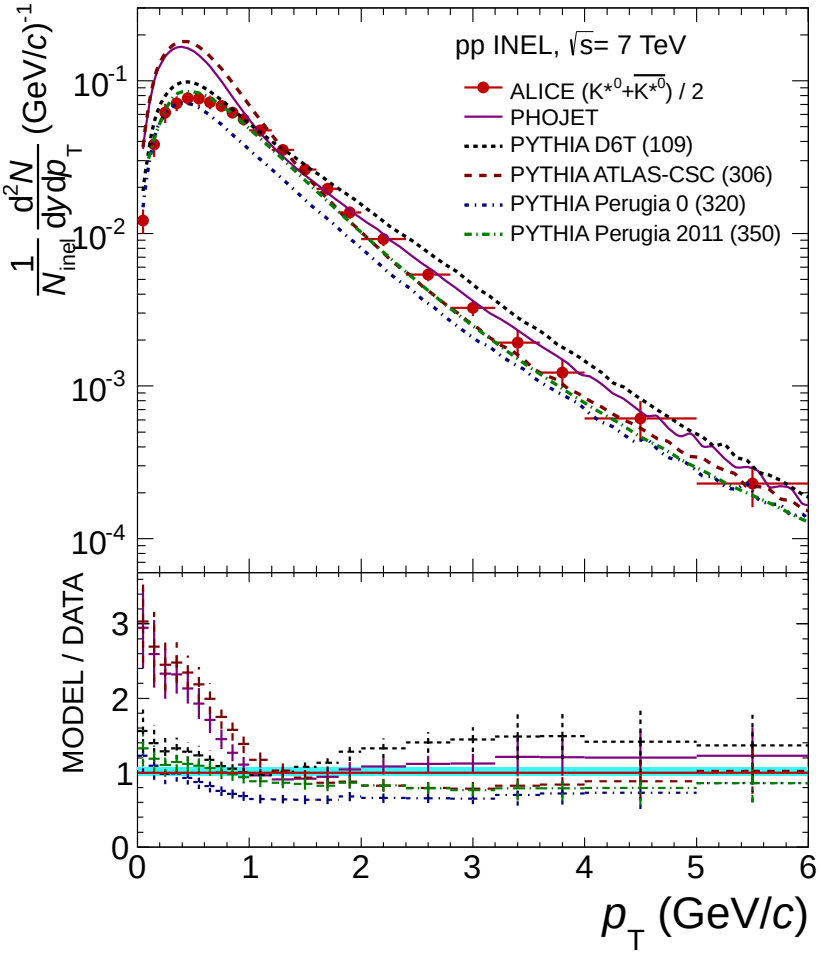


Fig. 8: (Colour online) Comparison of the K* $p_{\rm T}$ spectra in inelastic pp collisions with PHOJET and PYTHIA tunes D6T (109), ATLAS-CSC (306), Perugia 0 (320), and Perugia 2011 (350).

efficiency between data and Monte Carlo. The uncertainty on the yield contained in the extrapolated part of the ϕ spectrum was estimated to be $\pm$20% using different fit functions. The normalization to the number of inelastic collisions leads to a +6% and -3% uncertainty in the yield of the measured particles. The resulting overall systematic uncertainty is $^{+10}_{-9}$% ($^{+12.5}_{-11}$%) for the K* (ϕ) yield dN/dy and $\pm$2% (3%) for the average transverse momentum $\langle p_{\rm T} \rangle$.

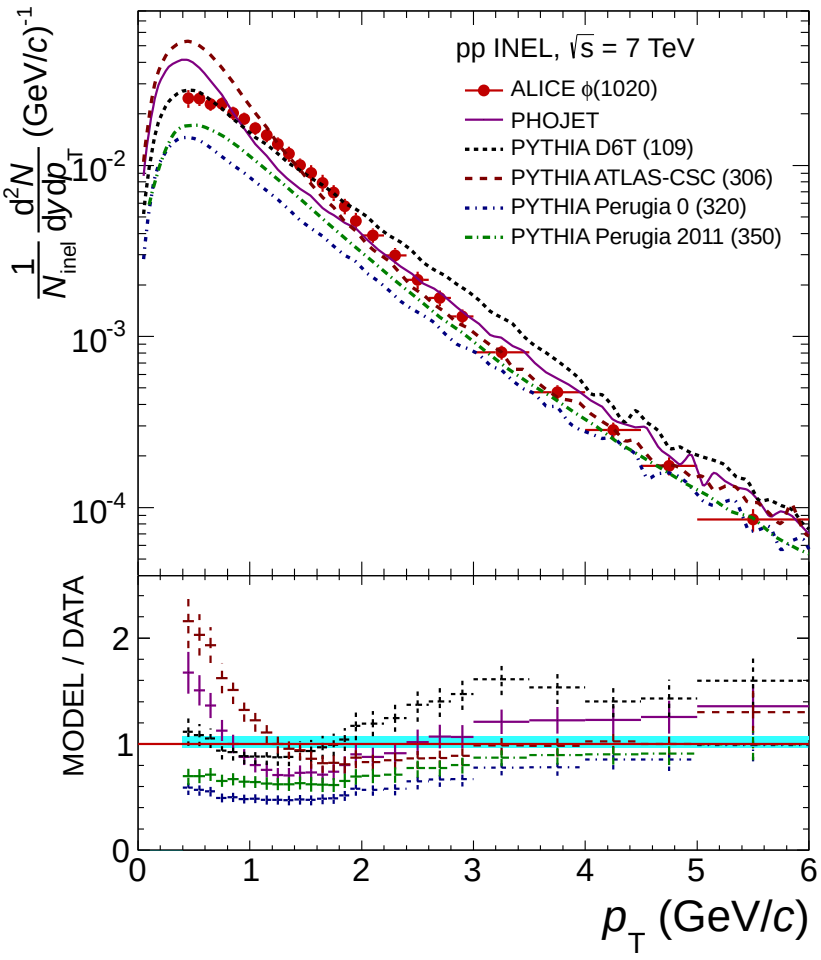


Fig. 9: (Colour online) Comparison of the $\phi(1020)$ p_{T} spectra in inelastic pp collisions with PHOJET and PYTHIA tunes D6T (109), ATLAS-CSC (306), Perugia 0 (320), and Perugia 2011 (350).

Table 2: Parameters extracted from the Lévy-Tsallis (4) fits to the K^* and ϕ transverse momentum spectra in 7 TeV pp collisions, including point-to-point systematic uncertainties. The first uncertainty is statistical and the second is systematic.

Particles	χ^2/ndf	T (MeV)	n
K^*	$2.0/19$	$254 \pm 2 \pm 18$	$6.2 \pm 0.07 \pm 0.8$
ϕ	$2.8/23$	$272 \pm 4 \pm 11$	$6.7 \pm 0.20 \pm 0.4$

Table 3: K^* and ϕ yield and $\langle p_{\mathrm{T}} \rangle$ estimated in the range 0-6 GeV/c in inelastic pp collisions at $\sqrt{s}$=7 TeV. The systematic uncertainties of dN/dy and $\langle p_{\mathrm{T}} \rangle$ include contributions from the choice of spectrum fit function for extrapolation, the absolute normalization, and the point-to-point uncertainties listed in Tab 1.

Particles	measured p_{T} (GeV/c)	dN/dy	$\langle p_{\mathrm{T}} \rangle$ (GeV/c)
K^*	$[0.0-6.0]$	$0.097 \pm 0.0004^{+0.010}_{-0.009}$	$1.01 \pm 0.003 \pm 0.02$
ϕ	$[0.4-6.0]$	$0.032 \pm 0.0004^{+0.004}_{-0.0035}$	$1.07 \pm 0.005 \pm 0.03$

5 Results and discussion

5.1 p_{T} spectra and integrated yield

Figure 6 presents the corrected p_{T} spectra for the two resonances. The statistical and point-to-point systematic uncertainties added in quadrature are shown. The spectra are fitted with a Lévy-Tsallis function [26, 27]

$$\frac{\mathrm{d}^2N}{\mathrm{d}y\mathrm{d}p_{\mathrm{T}}} = \frac{(n-1)(n-2)}{nT[nT+m(n-2)]} \times \frac{\mathrm{d}N}{\mathrm{d}y} \times p_{\mathrm{T}} \times \left(1+\frac{m_{\mathrm{T}}-m}{nT}\right)^{-n} \quad (4)$$

where $m_{\mathrm{T}} = \sqrt{m^2+p_{\mathrm{T}}^2}$. This function describes both the exponential shape of the spectrum at low p_{T} and the power-law distribution at large p_{T}, quantified by the inverse slope parameter T and the exponent parameter n, respectively. The extracted parameter values are listed in Table 2 and the fits are shown in Fig. 6. The χ^2/ndf values are smaller than unity because the point-to-point systematic uncertainties, which are included in the fit, could be correlated.

The extracted n values are similar to those quoted by the STAR experiment at RHIC for the ϕ measured in pp collisions at 200 GeV (n=8.3$\pm$1.2) [5]. In contrast, the slope parameters are significantly higher than the values obtained at RHIC, T= 202 $\pm$ 14 $\pm$ 11 MeV for ϕ, and T=223 $\pm$8$\pm$9 MeV for K^* [3] (the latter was obtained by an exponential fit and can therefore not be directly compared).

The total yields dN/dy and the mean transverse momentum $\langle p_{\mathrm{T}} \rangle$, including statistical and systematic uncertainties, are listed in Table 3. The values of dN/dy were obtained by integrating the spectra in the measured range and extrapolating to zero p_{T} with the fitted Lévy-Tsallis function. The contribution of the low-p_{T} extrapolation is negligible for the K^* and about 15 $\pm$ 3% for the ϕ. The mean transverse momentum was estimated in the range $0 < p_{\mathrm{T}} < 6$ GeV/c using the Lévy-Tsallis function. However, similar values are obtained when calculating the mean from the measured data points, using the fit only to extrapolate into the unmeasured p_{T} regions. In addition to the point to point systematic uncertainties previously described, an exponential fit was also used to estimate the systematic uncertainty in $\langle p_{\mathrm{T}} \rangle$ due to a different choice of fit function. Compared to pp collisions at 200 GeV [3, 5, 28], the mean p_{T} rises by about 30% (Fig. 7) and the yield per inelastic collision increases by about a factor of two, which is similar to the overall increase of charged particle multiplicity [29, 30].

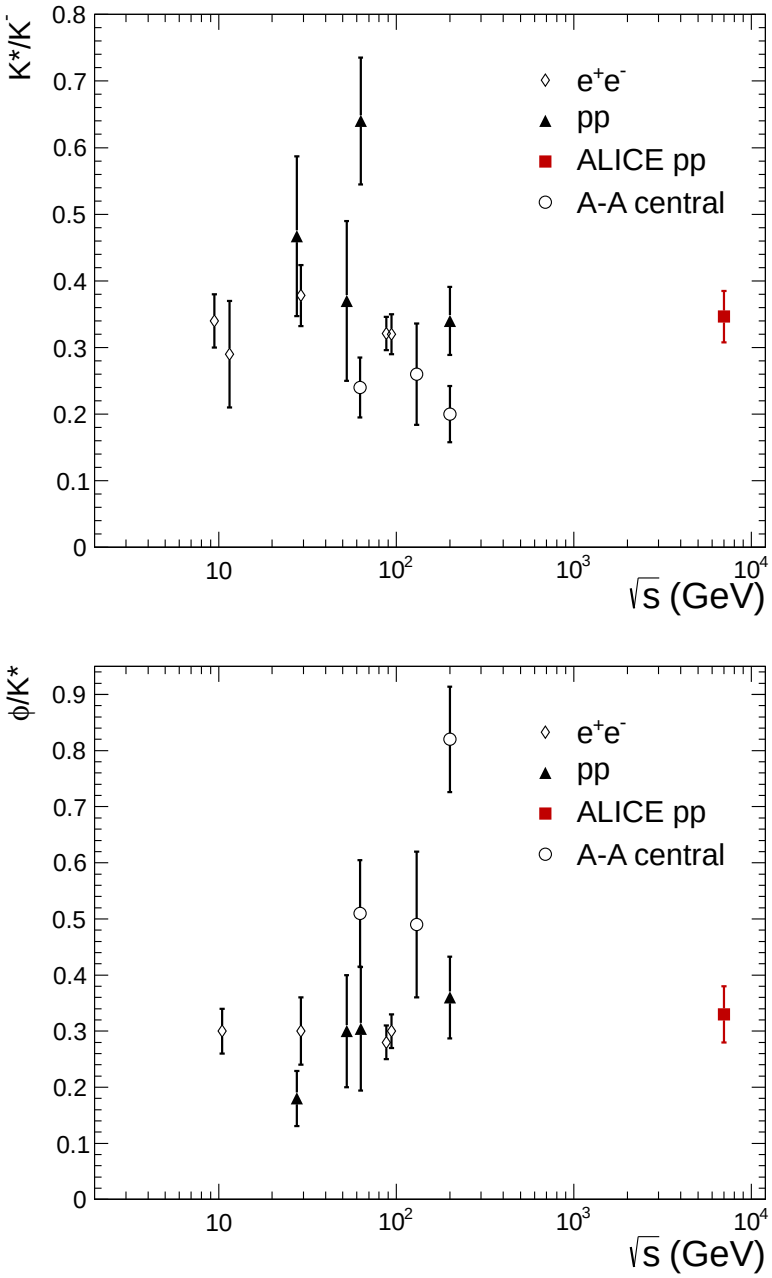


Fig. 10: (Colour online) Energy dependence of the K^*/K^- (upper panel) and ϕ/K^* (lower panel) ratio in e^+e^- (diamonds) [2, 41, 42, 46, 60], and pp (triangles) [1, 3, 5, 47, 48, 49] collisions. Red squares represent the data from the ALICE experiment for 7 TeV pp collisions, K^- yields are from [11]. Open circles represent the same ratios in central nucleus-nucleus collisions from [3, 5, 49, 50, 51]. Some points have been displaced horizontally for better visibility. Ratios are calculated from yields at mid-rapidity or in full phase space.

The ϕ yield, measured via the leptonic decay channel in the ALICE muon spectrometer in $2.5< y <4$, $1<p_T<5$ GeV/c [31], has a similar momentum distribution, but is lower by about 30% at forward rapidity. The ϕ yield is expected to vary by 20%-50% between forward ($2.5< y <4$) and mid-central ($-0.5< y <0.5$) rapidities, based on analysis of different PYTHIA tunes described in paragraph 5.2. In particular, the lower value is predicted from the D6T PYTHIA tune [35], which reproduces rather well the ϕ spectrum at forward rapidity [31] and the low p_T part of the ϕ spectrum at mid-rapidity (see Fig. 9 described in 5.2).

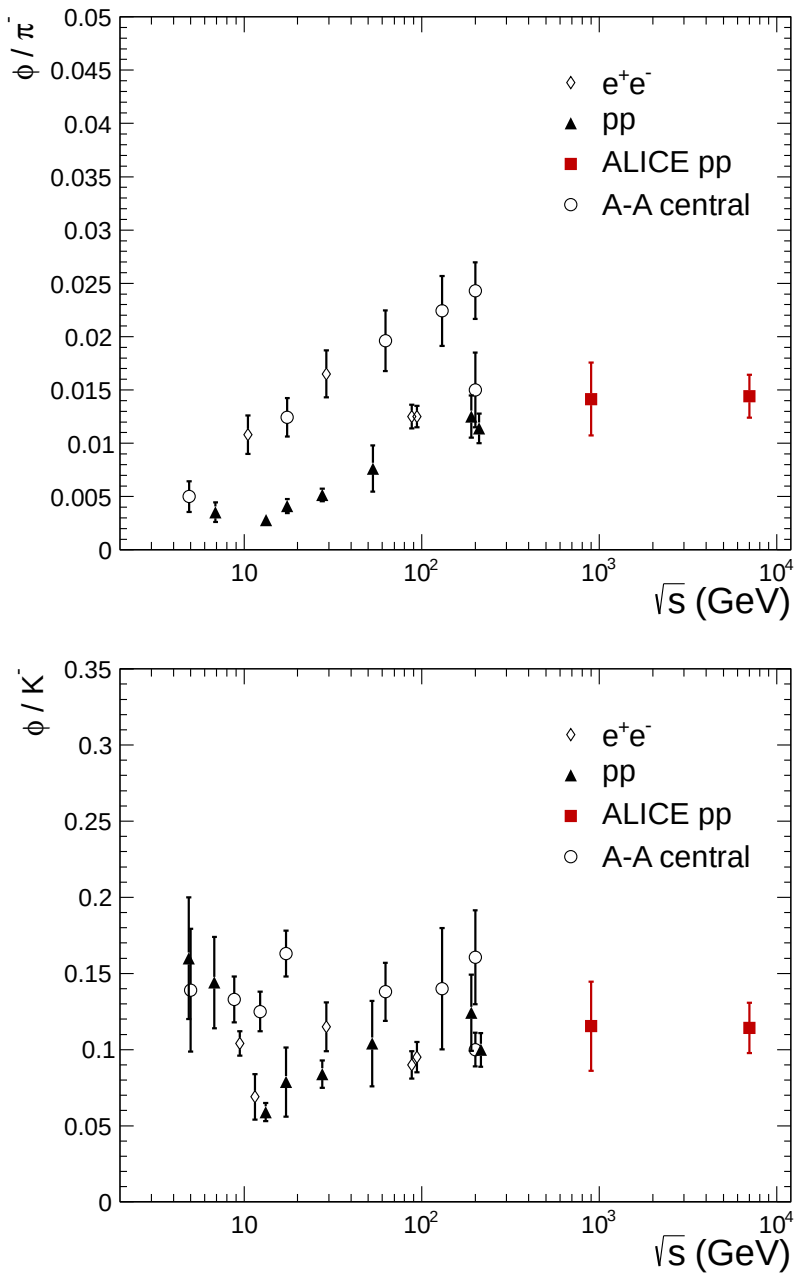


Fig. 11: (Colour online) Energy dependence of the ϕ/π^- (upper panel) and ϕ/K^- ratio (bottom panel) in nuclear (open circles) [4, 5, 50, 52, 53, 54, 55], e^+e^- (diamonds) [2, 41, 42, 46, 60], and pp (triangles) [1, 3, 5, 28, 45, 47, 52, 53, 54, 57] collisions. Other π^- and K^- yields are from [56, 57, 58, 59]. Red squares represent the ALICE data at 0.9 and 7 TeV. The pion and kaon yields at 7 TeV are from [11]. The ϕ, π^-, and K^- yields at 0.9 TeV are from [24, 32]. Some points have been displaced horizontally for better visibility. Ratios are calculated from yields at mid-rapidity or in full phase space, except the data at $\sqrt{s}$=4.87 GeV [52].

5.2 Comparisons to models

Multiparticle production, which is predominantly a soft, non-pertubative process, is usually modelled by QCD inspired Monte Carlo event generators like PHOJET [9] and PYTHIA [10]. In both models, hadronization is simulated using the Lund string fragmentation model [34]. Different PYTHIA tunes were obtained by adjusting the model parameters to reproduce existing data. The D6T tune [35], which uses the CTEQ6L parton distribution function (with a corresponding larger production of strange particles), was obtained by fitting CDF Run 2 data. The ATLAS-CSC [36] tune was adjusted to minimum bias data from the UA5, E735, and CDF experiments for energies ranging from 0.2 to 1.8 TeV. The latest PYTHIA tune, Perugia 2011 [14], takes into account first results from the LHC, in particular minimum-bias and underlying event data at 0.9 and 7 TeV. Strange baryon production was increased in this tune leading to a larger Λ/K ratio with respect to the Perugia 0 tune.

The transverse momentum spectra of K^* and ϕ are compared to PHOJET and various PYTHIA tunes in Figs. 8 and 9. For PYTHIA, tunes D6T (109), ATLAS-CSC (306), Perugia 0 (320) and Perugia 2011 (350) were used. The best agreement is found for the PYTHIA Perugia 2011 tune, which reproduces both the K^* spectrum and the high p_T part ($p_T > 3$ GeV/c) of the ϕ spectrum rather well. PHOJET and ATLAS-CSC very significantly overestimate the low momentum part ($p_T < 1$ GeV/c) of the transverse momentum distribution but reproduce the high momentum distribution of both mesons well. The PYTHIA D6T tune gives the best description at low p_T, but deviates from the data at $p_T > 2$ GeV/c. Finally, the PYTHIA Perugia 0 tune underestimates the meson yield for p_T larger than 0.5 GeV/c.

Similar comparisons for the mid- and forward-rapidity ϕ spectrum in pp collisions at $\sqrt{s}$=0.9 TeV [32] and 7 TeV [31], respectively, show that the ϕ spectrum is rather well reproduced by the ATLAS-CSC and D6T tunes, while the Perugia 0 and 2011 tunes underestimate the data. Moreover the PYTHIA tunes generally underestimate strange meson and hyperon production in 7 TeV pp collisions [12, 37], while the Perugia 2011 tune gives a good description of kaon production in pp collisions at 7 TeV [11].

5.3 Particle ratios

The measurement of particle production and particle ratios in pp collisions is important as a baseline for comparison with heavy ion reactions. In heavy ion collisions, the yields for stable and long-lived hadrons reflect the thermodynamic conditions (temperature, chemical potentials) at freeze-out, whereas the yield for short-lived resonances can be modified by final state interactions inside the hot and dense reaction zone [38, 39]. Particularly interesting is the comparison of ϕ and K^* production, considering the different lifetimes (about a factor 10) of the two resonances.

Using different particle ratios (like K/π or ϕ/K^*) measured in elementary collisions, values ranging from 0.1 to 0.4 [1, 2, 41, 42, 43] were previously obtained for the strange quark suppression factor $\lambda_s = 2s\bar{s}/(u\bar{u}+d\bar{d})$, which represents the probability to produce strange quark pairs relative to light quarks [40]. In pp reactions, particle abundances have been successfully described by statistical-thermal models. Now, using measured identified particle yields, an energy-independent value of 0.2 for λ_s has been extracted in e^+e^-, pp, and $p\bar{p}$ collisions at $\sqrt{s}<1$ TeV [40, 44].

Using the ϕ and K^* yields presented in this paper and stable particle results measured by ALICE at the same energy [11], we find the following values for particle ratios in pp collisions at 7 TeV: $K^*/K^- = 0.35 \pm 0.001$ (stat.) ± 0.04 (syst.), $\phi/K^* = 0.33 \pm 0.004$ (stat.) ± 0.05 (syst.), $\phi/K^- = 0.11 \pm 0.001$(stat.) ± 0.02 (syst.), $\phi/\pi^- = 0.014 \pm 0.0002$ (stat.) ± 0.002 (syst.). Due to the fact that the same data were analyzed to extract both resonance and non-resonance (π,K) yields, the uncertainties due to the absolute normalization cancel and are therefore not included in the systematic uncertainties of the ratios. These ratios are shown in Figures 10 and 11, together with the results obtained at lower incident energies in pp, e^+e^-, and A-A collisions.

The K^*/K^-, ϕ/K^-, and ϕ/K^* ratios are essentially independent of energy and also independent of the

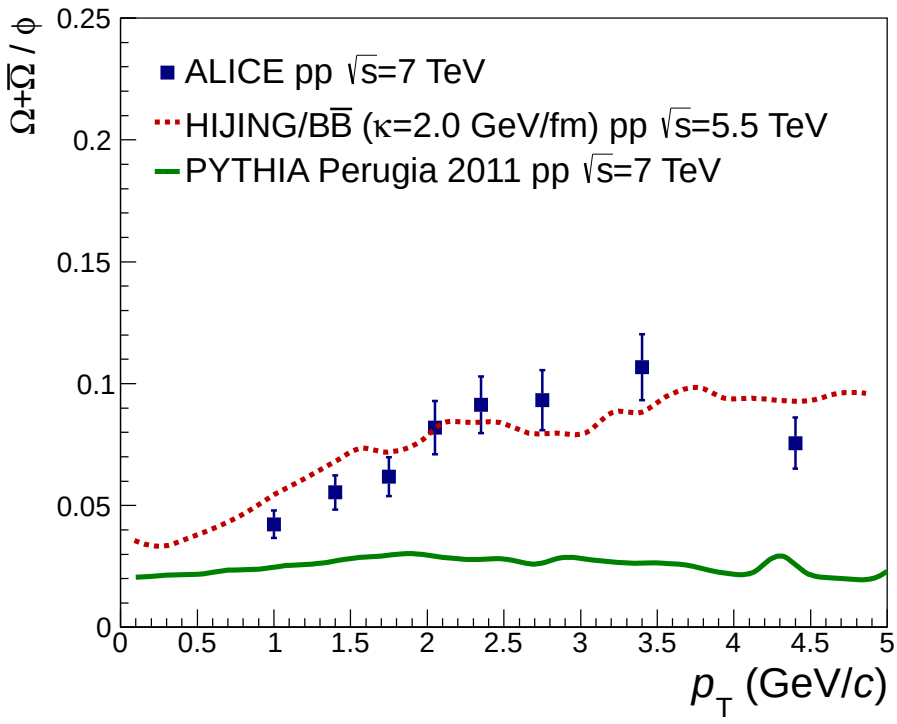


Fig. 12: (Colour online) $(\Omega^+ + \Omega^-)/\phi$ ratio as a function of transverse momentum for pp collisions at $\sqrt{s}$=7 TeV. Ω data are from [12]. The dashed line represents the prediction of HIJING/B$\overline{B}$ v2.0 model with a SCF for pp collisions at $\sqrt{s}$=5.5 TeV with a string tension of 2 GeV/fm [13]. The same calculation at 7 TeV yields a $\sim$ 10% higher ratio [62]. The full line represents the prediction of the PYTHIA Perugia 2011 tune [14] for pp collisions at $\sqrt{s}$=7 TeV.

collision system, with the exception of K^*/K and ϕ/K^* at RHIC [5, 49, 50, 51], where these ratios in nuclear collisions are respectively lower and higher than in pp. On the contrary, the ϕ/π ratio increases with energy both in heavy ion and in pp collisions up to at least 200 GeV. However, in heavy ion collisions the value obtained by the PHENIX experiment [4], about 40% lower than the STAR result [5] at the same collision energy, seems indicate a saturation of this ratio at the RHIC energies. In pp collisions we observe a saturation of the ϕ/π ratio, with no significant change over the LHC energy range between 1 and 7 TeV.

In microscopic models where soft particle production is governed by string fragmentation, strange hadron yields are predicted to depend on the string tension [8]. Multi-strange baryons, and in particular the ratio Ω/ϕ, are expected to be very sensitive to this effect [13]. The ϕ yield is compared to the $\Omega^- + \overline{\Omega}^+$ data measured by ALICE at the same incident energy [12] in Fig. 12 as a function of transverse momentum. The full line represents the PYTHIA model (Perugia 2011 tune), which is a factor 1.5-5 below the data. While this tune describes the ϕ spectrum reasonably well above 2-3 GeV/c, it underpredicts multistrange baryon yields by a large factor [12]. The dashed line, which is very close to the data, represents the prediction of a model with increased string tension, the HIJING/B$\overline{\text{B}}$ v2.0 model with a Strong Colour Field (SCF), for pp collisions at 5.5 TeV [13]. This is a model that combines multiple minijet production via perturbative QCD with soft longitudinal string excitation and hadronization. In this case the SCF effects are modeled by varying the effective string tensions that controls the $q\overline{q}$ and $qq\overline{qq}$ pair creation rates and the strangeness suppression factor. The value of string tension used in this calculation is κ=2 GeV/fm, equal to the value used to fit the high baryon/meson ratio at $\sqrt{s}$=1.8 TeV reported by the CDF collaboration [61]. The same calculation at 7 TeV yields a $\sim$ 10% higher ratio [62]. Higher values of the string tension ($\sim$ 3 GeV/fm) also successfully reproduce also the $(\Omega+\overline{\Omega})/\phi$ ratio in Au-Au collisions at $\sqrt{s}$=200 GeV [13], but overestimate the $(\Lambda+\overline{\Lambda})/K^0_S$ at 7 TeV [8].

6 Conclusion

Yields and spectra of $K^*(892)^0$ and $\phi(1020)$ mesons were measured for inelastic pp collisions at $\sqrt{s}$=7 TeV by the ALICE collaboration at the LHC. The transverse momentum spectra are well described by the Lévy-Tsallis function. The yields for both mesons increase by about a factor of two from 200 GeV centre-of-mass energy, and the average $p_{\rm T}$ by about 30%.

The K^*/K and ϕ/K^* ratios (and consequently the ϕ/K ratio) are found to be independent of energy up to 7 TeV. Also the ϕ/π ratio, which increases in both pp and A-A collisions up to at least RHIC energies, saturates and becomes independent of energy above 200 GeV.

The data have been compared to a number of PYTHIA tunes and the PHOJET event generator. None of them gives a fully satisfactory description of the data. The latest PYTHIA version (Perugia 2011) comes closest, while still underpredicting the ϕ meson $p_{\rm T}$ spectrum below 3 GeV/c by up to a factor of two.

The $(\Omega^- + \overline{\Omega}^+)/\phi$ ratio is not reproduced by PYTHIA Perugia 2011, but is in good agreement with the HIJING/B$\overline{\text{B}}$ v2.0 model with SCF, which enhances multi-strange baryon production by increasing the string tension parameter.

References

[1] M. Aguilar-Benitez et al. (LEBC-EHS Collaboration) Z. Phys. C **50** (1991) 405.

[2] H. Albrecht et al., Z. Phys. C**61** (1994) 1.

[3] J. Adams et al. (STAR Collaboration), Phys. Rev. C **71** (2005) 064902.

[4] S.S. Adler et al. (PHENIX Collaboration), Phys. Rev. C **72** (2005) 014903.

[5] B.I. Abelev et al. (STAR Collaboration), Phys. Rev. C **79** (2009) 064903.

[6] P.K. Malhotra and R. Orava, Z. Phys. C **17** (1983) 85.

[7] A. Wroblewski, Acta Phys. Pol. B **16** (1985) 379.

[8] V. Topor Pop et al., Phys. Rev. C **83** (2011) 024902.

[9] R. Engel et al., Z. Phys. C **66** (1995) 203; R. Engel and J. Ranft, Phys. Rev. D **54** (1996) 4244.

[10] T. Sjöstrand, S. Mrenna and P. Skands, J. High Energy Phys. **05** (2006) 026.

[11] B. Abelev et al. (ALICE Collaboration), Measurement of pion, kaon and proton production in pp collisions at 7 TeV, in preparation.

[12] B. Abelev et al. (ALICE Collaboration), Phys. Lett. B **712** (2012) 309.

[13] N. Armesto et al., J. Phys. G: Nucl. Part. Phys. **35** (2008) 054001.

[14] P.Z. Skands, Phys. Rev. D **82** (2010) 074018.

[15] K. Aamodt et al. (ALICE Collaboration) J. Instrum. **3** (2008) S08002.

[16] K. Aamodt et al. (ALICE Collaboration), J. Instrum. **5** (2010) P03003.

[17] J. Alme et al., Nucl. Instr. Meth. in Phys. Res. A **622** (2010) 316.

[18] A. Akindinov et al., Nuovo Cim. B **124** (2009) 235.

[19] A. Akindinov et al., Eur. Phys. J. C **68** (2010) 601.

[20] B. Abelev et al. (ALICE Collaboration), Measurement of inelastic, single- and double-diffraction cross sections in proton-proton collisions at LHC with ALICE, arXiv:1208.4968v1.

[21] K. Aamodt et al. (ALICE Collaboration), Eur. Phys. J. C **65**, (2010) 111.

[22] B. Alessandro et al. (ALICE Collaboration), J. Phys. G Nucl. Part. Phys. **32**, (2006) 1295.

[23] W. Blum, W. Riegler, and L. Rolandi, *Particle Detection with Drift Chambers*, 2nd ed. (Springer Verlag, 2008).

[24] K. Aamodt et al. (ALICE Collaboration), Eur. Phys. J. C **71** (2011) 1655.

[25] K. Nakamura et al. (Particle Data Group), J. Phys. G **37** (2010) 075021 and 2011 partial update for the 2012 edition.

[26] C. Tsallis, J. Stat. Phys. **52** (1988) 479.

[27] B.I. Abelev et al. (STAR Collaboration), Phys. Rev. C **75** (2007) 064901.

[28] A. Adare et al., (PHENIX Collaboration), Phys. Rev. D **83** (2011) 052004.

[29] K. Aamodt et al. (ALICE Collaboration), Eur. Phys. J. C **68** (2010) 89.

[30] K. Aamodt et al. (ALICE Collaboration), Eur. Phys. J. C **68** (2010) 345.

[31] B. Abelev et al. (ALICE Collaboration), Phys. Lett. B **710** (2012) 557.

[32] K. Aamodt et al. (ALICE Collaboration), Eur. Phys. J. C **71** (2011) 1594.

[33] T. Alexopoulos et al. (E735 Collaboration), Z. Phys. C **67** (1995) 411.

[34] B. Andersson et al., Phys. Rep. **97** (1983) 31.

[35] R. Field, Acta Phys. Pol. B **39** (2008) 2611; R. Field, arXiv:1003.4220.

[36] C. Buttar et al., Acta Phys. Pol. B **35** (2004) 43.

[37] S. Chatrchyan et al. (CMS Collaboration), J. High Energy Phys. **08** (2011) 086.

[38] C. Markert, J. Phys. G: Nucl. Part. Phys. **31** (2005) S897.

[39] M. Bleicher and J. Aichelin, Phys. Lett. B **530** (2002) 81.

[40] F. Becattini, M. Gazdzicki, J. Sollfrank, Eur. Phys. J. C **5** (1998) 143.

[41] Y. Pei, Z. Phys. C **72** (1996) 39.

[42] H. Hofmann et al., Ann. Rev. Nucl. Part. Sci. **38** (1988) 279.

[43] C. Bocquet et al., Phys. Lett. B **366** (1996) 447.

[44] F. Becattini, J. Cleymans, K. Redlich, Phys. Rev. C **64** (2001) 024901.

[45] V. Blobel et al., Phys. Lett. **B59** (1975) 88.

[46] K. Abe et al., Phys. Rev. D **59** (1999) 052001.
[47] D. Drijard et al., Z. Phys. C **9** (1981) 293.
[48] T. Akesson et al., Nucl. Phys. B **203** (1982) 27.
[49] M.M. Aggarwal et al. (STAR Collaboration), Phys. Rev. C **84** (2011) 034909.
[50] C. Adler et al. (STAR Collaboration), Phys. Rev. C **65** (2002) 041901.
[51] C. Adler et al. (STAR Collaboration), Phys. Rev. C **66** (2002) 061901.
[52] B.B. Back et al., (E917 Collaboration), Phys. Rev. C **69** (2004) 054901.
[53] S.V. Afanasiev et al. (NA49 Collaboration), Phys. Lett. B **491** (2000) 59.
[54] C. Alt et al. (NA49 Collaboration), Phys. Rev. C **78** (2008) 044907.
[55] K. Adcox et al. (PHENIX Collaboration), Phys. Rev. Lett. **88** (2002) 242301.
[56] J. Adams et al. (STAR Collaboration), Phys. Rev. Lett. **92** (2004) 112301.
[57] C. Daum et al., Nucl. Phys. B **186** (1981) 205.
[58] A.M. Rossi et al., Nucl. Phys. B **84** (1975) 269.
[59] A. Adare et al. (PHENIX Collaboration), Phys. Rev. C **83**, (2011) 064903.
[60] S. Behrends et al., Phys. Rev. D **31** (1985) 2161.
[61] D. Acosta et al. (CDF Collaboration), Phys. Rev. D **72** (2005) 052001.
[62] V. Topor Pop, private communication.

7 Acknowledgements

The ALICE collaboration would like to thank all its engineers and technicians for their invaluable contributions to the construction of the experiment and the CERN accelerator teams for the outstanding performance of the LHC complex.
The ALICE collaboration acknowledges the following funding agencies for their support in building and running the ALICE detector:
Calouste Gulbenkian Foundation from Lisbon and Swiss Fonds Kidagan, Armenia;
Conselho Nacional de Desenvolvimento Científico e Tecnológico (CNPq), Financiadora de Estudos e Projetos (FINEP), Fundação de Amparo à Pesquisa do Estado de São Paulo (FAPESP);
National Natural Science Foundation of China (NSFC), the Chinese Ministry of Education (CMOE) and the Ministry of Science and Technology of China (MSTC);
Ministry of Education and Youth of the Czech Republic;
Danish Natural Science Research Council, the Carlsberg Foundation and the Danish National Research Foundation;
The European Research Council under the European Community's Seventh Framework Programme;
Helsinki Institute of Physics and the Academy of Finland;
French CNRS-IN2P3, the 'Region Pays de Loire', 'Region Alsace', 'Region Auvergne' and CEA, France;
German BMBF and the Helmholtz Association;
General Secretariat for Research and Technology, Ministry of Development, Greece;
Hungarian OTKA and National Office for Research and Technology (NKTH);
Department of Atomic Energy and Department of Science and Technology of the Government of India;
Istituto Nazionale di Fisica Nucleare (INFN) of Italy;
MEXT Grant-in-Aid for Specially Promoted Research, Japan;
Joint Institute for Nuclear Research, Dubna;
National Research Foundation of Korea (NRF);
CONACYT, DGAPA, México, ALFA-EC and the HELEN Program (High-Energy physics Latin-American–European Network);
Stichting voor Fundamenteel Onderzoek der Materie (FOM) and the Nederlandse Organisatie voor

Wetenschappelijk Onderzoek (NWO), Netherlands;
Research Council of Norway (NFR);
Polish Ministry of Science and Higher Education;
National Authority for Scientific Research - NASR (Autoritatea Naţională pentru Cercetare Ştiinţifică - ANCS);
Federal Agency of Science of the Ministry of Education and Science of Russian Federation, International Science and Technology Center, Russian Academy of Sciences, Russian Federal Agency of Atomic Energy, Russian Federal Agency for Science and Innovations and CERN-INTAS;
Ministry of Education of Slovakia;
Department of Science and Technology, South Africa;
CIEMAT, EELA, Ministerio de Educación y Ciencia of Spain, Xunta de Galicia (Consellería de Educación), CEADEN, Cubaenergía, Cuba, and IAEA (International Atomic Energy Agency);
Swedish Research Council (VR) and Knut & Alice Wallenberg Foundation (KAW);
Ukraine Ministry of Education and Science;
United Kingdom Science and Technology Facilities Council (STFC);
The United States Department of Energy, the United States National Science Foundation, the State of Texas, and the State of Ohio.

A The ALICE Collaboration

B. Abelev[68] , J. Adam[33] , D. Adamová[73] , A.M. Adare[120] , M.M. Aggarwal[77] , G. Aglieri Rinella[29] , A.G. Agocs[60] , A. Agostinelli[18] , S. Aguilar Salazar[56] , Z. Ahammed[116] , N. Ahmad[13] , A. Ahmad Masoodi[13] , S.A. Ahn[62] , S.U. Ahn[36] , A. Akindinov[46] , D. Aleksandrov[88] , B. Alessandro[94] , R. Alfaro Molina[56] , A. Alici[97 ,9] , A. Alkin[2] , E. Almaráz Aviña[56] , J. Alme[31] , T. Alt[35] , V. Altini[27] , S. Altinpinar[14] , I. Altsybeev[117] , C. Andrei[70] , A. Andronic[85] , V. Anguelov[82] , J. Anielski[54] , C. Anson[15] , T. Antičić[86] , F. Antinori[93] , P. Antonioli[97] , L. Aphecetche[102] , H. Appelshäuser[52] , N. Arbor[64] , S. Arcelli[18] , A. Arend[52] , N. Armesto[12] , R. Arnaldi[94] , T. Aronsson[120] , I.C. Arsene[85] , M. Arslandok[52] , A. Asryan[117] , A. Augustinus[29] , R. Averbeck[85] , T.C. Awes[74] , J. Äystö[37] , M.D. Azmi[13] , M. Bach[35] , A. Badalà[99] , Y.W. Baek[63 ,36] , R. Bailhache[52] , R. Bala[94] , R. Baldini Ferroli[9] , A. Baldisseri[11] , A. Baldit[63] , F. Baltasar Dos Santos Pedrosa[29] , J. Bán[47] , R.C. Baral[48] , R. Barbera[24] , F. Barile[27] , G.G. Barnaföldi[60] , L.S. Barnby[90] , V. Barret[63] , J. Bartke[104] , M. Basile[18] , N. Bastid[63] , S. Basu[116] , B. Bathen[54] , G. Batigne[102] , B. Batyunya[59] , C. Baumann[52] , I.G. Bearden[71] , H. Beck[52] , I. Belikov[58] , F. Bellini[18] , R. Bellwied[110] , E. Belmont-Moreno[56] , G. Bencedi[60] , S. Beole[22] , I. Berceanu[70] , A. Bercuci[70] , Y. Berdnikov[75] , D. Berenyi[60] , A.A.E. Bergognon[102] , D. Berzano[94] , L. Betev[29] , A. Bhasin[80] , A.K. Bhati[77] , J. Bhom[114] , N. Bianchi[65] , L. Bianchi[22] , C. Bianchin[19] , J. Bielčík[33] , J. Bielčíková[73] , A. Bilandzic[72 ,71] , S. Bjelogrlic[45] , F. Blanco[110] , F. Blanco[7] , D. Blau[88] , C. Blume[52] , M. Boccioli[29] , N. Bock[15] , S. Böttger[51] , A. Bogdanov[69] , H. Bøggild[71] , M. Bogolyubsky[43] , L. Boldizsár[60] , M. Bombara[34] , J. Book[52] , H. Borel[11] , A. Borissov[119] , S. Bose[89] , F. Bossú[22] , M. Botje[72] , B. Boyer[42] , E. Braidot[67] , P. Braun-Munzinger[85] , M. Bregant[102] , T. Breitner[51] , T.A. Browning[83] , M. Broz[32] , R. Brun[29] , E. Bruna[22 ,94] , G.E. Bruno[27] , D. Budnikov[87] , H. Buesching[52] , S. Bufalino[22 ,94] , O. Busch[82] , Z. Buthelezi[79] , D. Caballero Orduna[120] , D. Caffarri[19] , X. Cai[39] , H. Caines[120] , E. Calvo Villar[91] , P. Camerini[20] , V. Canoa Roman[8] , G. Cara Romeo[97] , F. Carena[29] , W. Carena[29] , N. Carlin Filho[107] , F. Carminati[29] , A. Casanova Díaz[65] , J. Castillo Castellanos[11] , J.F. Castillo Hernandez[85] , E.A.R. Casula[21] , V. Catanescu[70] , C. Cavicchioli[29] , C. Ceballos Sanchez[6] , J. Cepila[33] , P. Cerello[94] , B. Chang[37 ,123] , S. Chapeland[29] , J.L. Charvet[11] , S. Chattopadhyay[116] , S. Chattopadhyay[89] , I. Chawla[77] , M. Cherney[76] , C. Cheshkov[29 ,109] , B. Cheynis[109] , V. Chibante Barroso[29] , D.D. Chinellato[108] , P. Chochula[29] , M. Chojnacki[45] , S. Choudhury[116] , P. Christakoglou[72] , C.H. Christensen[71] , P. Christiansen[28] , T. Chujo[114] , S.U. Chung[84] , C. Cicalo[96] , L. Cifarelli[18 ,29 ,9] , F. Cindolo[97] , J. Cleymans[79] , F. Coccetti[9] , F. Colamaria[27] , D. Colella[27] , G. Conesa Balbastre[64] , Z. Conesa del Valle[29] , P. Constantin[82] , G. Contin[20] , J.G. Contreras[8] , T.M. Cormier[119] , Y. Corrales Morales[22] , P. Cortese[26] , I. Cortés Maldonado[1] , M.R. Cosentino[67] , F. Costa[29] , M.E. Cotallo[7] , E. Crescio[8] , P. Crochet[63] , E. Cruz Alaniz[56] , E. Cuautle[55] , L. Cunqueiro[65] , A. Dainese[19 ,93] , H.H. Dalsgaard[71] , A. Danu[50] , D. Das[89] , K. Das[89] , I. Das[42] , A. Dash[108] , S. Dash[40] , S. De[116] , G.O.V. de Barros[107] , A. De Caro[25 ,9] , G. de Cataldo[98] , J. de Cuveland[35] , A. De Falco[21] , D. De Gruttola[25] , H. Delagrange[102] , A. Deloff[100] , V. Demanov[87] , N. De Marco[94] , E. Dénes[60] , S. De Pasquale[25] , A. Deppman[107] , G. D Erasmo[27] , R. de Rooij[45] , M.A. Diaz Corchero[7] , D. Di Bari[27] , C. Di Giglio[27] , T. Dietel[54] , S. Di Liberto[95] , A. Di Mauro[29] , P. Di Nezza[65] , R. Divià[29] , Ø. Djuvsland[14] , A. Dobrin[119 ,28] , T. Dobrowolski[100] , I. Domínguez[55] , B. Dönigus[85] , O. Dordic[17] , O. Driga[102] , A.K. Dubey[116] , A. Dubla[45] , L. Ducroux[109] , P. Dupieux[63] , A.K. Dutta Majumdar[89] , M.R. Dutta Majumdar[116] , D. Elia[98] , D. Emschermann[54] , H. Engel[51] , B. Erazmus[102] , H.A. Erdal[31] , B. Espagnon[42] , M. Estienne[102] , S. Esumi[114] , D. Evans[90] , G. Eyyubova[17] , D. Fabris[19 ,93] , J. Faivre[64] , D. Falchieri[18] , A. Fantoni[65] , M. Fasel[85] , R. Fearick[79] , A. Fedunov[59] , D. Fehlker[14] , L. Feldkamp[54] , D. Felea[50] , B. Fenton-Olsen[67] , G. Feofilov[117] , A. Fernández Téllez[1] , R. Ferretti[26] , A. Ferretti[22] , A. Festanti[19] , J. Figiel[104] , M.A.S. Figueredo[107] , S. Filchagin[87] , D. Finogeev[44] , F.M. Fionda[27] , E.M. Fiore[27] , M. Floris[29] , S. Foertsch[79] , P. Foka[85] , S. Fokin[88] , E. Fragiacomo[92] , A. Francescon[29 ,19] , U. Frankenfeld[85] , U. Fuchs[29] , C. Furget[64] , M. Fusco Girard[25] , J.J. Gaardhøje[71] , M. Gagliardi[22] , A. Gago[91] , M. Gallio[22] , D.R. Gangadharan[15] , P. Ganoti[74] , C. Garabatos[85] , E. Garcia-Solis[10] , I. Garishvili[68] , J. Gerhard[35] , M. Germain[102] , C. Geuna[11] , M. Gheata[50 ,29] , A. Gheata[29] , B. Ghidini[27] , P. Ghosh[116] , P. Gianotti[65] , M.R. Girard[118] , P. Giubellino[29] , E. Gladysz-Dziadus[104] , P. Glässel[82] , R. Gomez[106] , E.G. Ferreiro[12] , L.H. González-Trueba[56] , P. González-Zamora[7] , S. Gorbunov[35] , A. Goswami[81] , S. Gotovac[103] , V. Grabski[56] , L.K. Graczykowski[118] , R. Grajcarek[82] , A. Grelli[45] , C. Grigoras[29] , A. Grigoras[29] , V. Grigoriev[69] , S. Grigoryan[59] , A. Grigoryan[121] , B. Grinyov[2] , N. Grion[92] , P. Gros[28] , J.F. Grosse-Oetringhaus[29] , J.-Y. Grossiord[109] , R. Grosso[29] , F. Guber[44] , R. Guernane[64] , C. Guerra Gutierrez[91] , B. Guerzoni[18] , M. Guilbaud[109] , K. Gulbrandsen[71] , T. Gunji[113] , R. Gupta[80] , A. Gupta[80] , H. Gutbrod[85] , Ø. Haaland[14] , C. Hadjidakis[42] , M. Haiduc[50] , H. Hamagaki[113] , G. Hamar[60] , B.H. Han[16] , L.D. Hanratty[90] , A. Hansen[71] , Z. Harmanova[34] , J.W. Harris[120] , M. Hartig[52] , D. Hasegan[50] , D. Hatzifotiadou[97] , A. Hayrapetyan[29 ,121] , S.T. Heckel[52] , M. Heide[54] , H. Helstrup[31] , A. Herghelegiu[70] , G. Herrera Corral[8] , N. Herrmann[82] , B.A. Hess[115] , K.F. Hetland[31] , B. Hicks[120] , P.T. Hille[120] , B. Hippolyte[58] , T. Horaguchi[114] , Y. Hori[113] ,

P. Hristov[29] , I. Hřivnáčová[42] , M. Huang[14] , T.J. Humanic[15] , D.S. Hwang[16] , R. Ichou[63] , R. Ilkaev[87] , I. Ilkiv[100] , M. Inaba[114] , E. Incani[21] , G.M. Innocenti[22] , P.G. Innocenti[29] , M. Ippolitov[88] , M. Irfan[13] , C. Ivan[85] , V. Ivanov[75] , A. Ivanov[117] , M. Ivanov[85] , O. Ivanytskyi[2] , A. Jachołkowski[24] , P. M. Jacobs[67] , H.J. Jang[62] , R. Janik[32] , M.A. Janik[118] , P.H.S.Y. Jayarathna[110] , S. Jena[40] , D.M. Jha[119] , R.T. Jimenez Bustamante[55] , L. Jirden[29] , P.G. Jones[90] , H. Jung[36] , A. Jusko[90] , A.B. Kaidalov[46] , V. Kakoyan[121] , S. Kalcher[35] , P. Kaliňák[47] , T. Kalliokoski[37] , A. Kalweit[53 ,29] , J.H. Kang[123] , V. Kaplin[69] , A. Karasu Uysal[29 ,122] , O. Karavichev[44] , T. Karavicheva[44] , E. Karpechev[44] , A. Kazantsev[88] , U. Kebschull[51] , R. Keidel[124] , M.M. Khan[13] , S.A. Khan[116] , P. Khan[89] , A. Khanzadeev[75] , Y. Kharlov[43] , B. Kileng[31] , M.Kim[36] , B. Kim[123] , S. Kim[16] , S.H. Kim[36] , T. Kim[123] , M. Kim[123] , D.J. Kim[37] , J.S. Kim[36] , J.H. Kim[16] , D.W. Kim[36] , S. Kirsch[35] , I. Kisel[35] , S. Kiselev[46] , A. Kisiel[118] , J.L. Klay[4] , J. Klein[82] , C. Klein-Bösing[54] , M. Kliemant[52] , A. Kluge[29] , M.L. Knichel[85] , A.G. Knospe[105] , K. Koch[82] , M.K. Köhler[85] , T. Kollegger[35] , A. Kolojvari[117] , V. Kondratiev[117] , N. Kondratyeva[69] , A. Konevskikh[44] , A. Korneev[87] , R. Kour[90] , M. Kowalski[104] , S. Kox[64] , G. Koyithatta Meethaleveedu[40] , J. Kral[37] , I. Králik[47] , F. Kramer[52] , I. Kraus[85] , T. Krawutschke[82 ,30] , M. Krelina[33] , M. Kretz[35] , M. Krivda[90 ,47] , F. Krizek[37] , M. Krus[33] , E. Kryshen[75] , M. Krzewicki[85] , Y. Kucheriaev[88] , T. Kugathasan[29] , C. Kuhn[58] , P.G. Kuijer[72] , I. Kulakov[52] , J. Kumar[40] , P. Kurashvili[100] , A. Kurepin[44] , A.B. Kurepin[44] , A. Kuryakin[87] , V. Kushpil[73] , S. Kushpil[73] , H. Kvaerno[17] , M.J. Kweon[82] , Y. Kwon[123] , P. Ladrón de Guevara[55] , I. Lakomov[42] , R. Langoy[14] , S.L. La Pointe[45] , C. Lara[51] , A. Lardeux[102] , P. La Rocca[24] , C. Lazzeroni[90] , R. Lea[20] , Y. Le Bornec[42] , M. Lechman[29] , K.S. Lee[36] , G.R. Lee[90] , S.C. Lee[36] , F. Lefèvre[102] , J. Lehnert[52] , L. Leistam[29] , V. Lenti[98] , H. León[56] , M. Leoncino[94] , I. León Monzón[106] , H. León Vargas[52] , P. Lévai[60] , J. Lien[14] , R. Lietava[90] , S. Lindal[17] , V. Lindenstruth[35] , C. Lippmann[85 ,29] , M.A. Lisa[15] , L. Liu[14] , V.R. Loggins[119] , V. Loginov[69] , S. Lohn[29] , D. Lohner[82] , C. Loizides[67] , K.K. Loo[37] , X. Lopez[63] , E. López Torres[6] , G. Løvhøiden[17] , X.-G. Lu[82] , P. Luettig[52] , M. Lunardon[19] , J. Luo[39] , G. Luparello[45] , L. Luquin[102] , C. Luzzi[29] , R. Ma[120] , K. Ma[39] , D.M. Madagodahettige-Don[110] , A. Maevskaya[44] , M. Mager[53 ,29] , D.P. Mahapatra[48] , A. Maire[82] , M. Malaev[75] , I. Maldonado Cervantes[55] , L. Malinina[59 ,,i], D. Mal'Kevich[46] , P. Malzacher[85] , A. Mamonov[87] , L. Manceau[94] , L. Mangotra[80] , V. Manko[88] , F. Manso[63] , V. Manzari[98] , Y. Mao[39] , M. Marchisone[63 ,22] , J. Mareš[49] , G.V. Margagliotti[20 ,92] , A. Margotti[97] , A. Marín[85] , C.A. Marin Tobon[29] , C. Markert[105] , I. Martashvili[112] , P. Martinengo[29] , M.I. Martínez[1] , A. Martínez Davalos[56] , G. Martínez García[102] , Y. Martynov[2] , A. Mas[102] , S. Masciocchi[85] , M. Masera[22] , A. Masoni[96] , L. Massacrier[102] , A. Mastroserio[27] , Z.L. Matthews[90] , A. Matyja[104 ,102] , C. Mayer[104] , J. Mazer[112] , M.A. Mazzoni[95] , F. Meddi[23] , A. Menchaca-Rocha[56] , J. Mercado Pérez[82] , M. Meres[32] , Y. Miake[114] , L. Milano[22] , J. Milosevic[17 ,,ii], A. Mischke[45] , A.N. Mishra[81] , D. Miśkowiec[85 ,29] , C. Mitu[50] , J. Mlynarz[119] , B. Mohanty[116] , L. Molnar[60 ,29] , L. Montaño Zetina[8] , M. Monteno[94] , E. Montes[7] , T. Moon[123] , M. Morando[19] , D.A. Moreira De Godoy[107] , S. Moretto[19] , A. Morsch[29] , V. Muccifora[65] , E. Mudnic[103] , S. Muhuri[116] , M. Mukherjee[116] , H. Müller[29] , M.G. Munhoz[107] , L. Musa[29] , A. Musso[94] , B.K. Nandi[40] , R. Nania[97] , E. Nappi[98] , C. Nattrass[112] , N.P. Naumov[87] , S. Navin[90] , T.K. Nayak[116] , S. Nazarenko[87] , G. Nazarov[87] , A. Nedosekin[46] , M. Nicassio[27] , M.Niculescu[50 ,29] , B.S. Nielsen[71] , T. Niida[114] , S. Nikolaev[88] , V. Nikolic[86] , V. Nikulin[75] , S. Nikulin[88] , B.S. Nilsen[76] , M.S. Nilsson[17] , F. Noferini[97 ,9] , P. Nomokonov[59] , G. Nooren[45] , N. Novitzky[37] , A. Nyanin[88] , A. Nyatha[40] , C. Nygaard[71] , J. Nystrand[14] , A. Ochirov[117] , H. Oeschler[53 ,29] , S.K. Oh[36] , S. Oh[120] , J. Oleniacz[118] , C. Oppedisano[94] , A. Ortiz Velasquez[28 ,55] , G. Ortona[22] , A. Oskarsson[28] , P. Ostrowski[118] , J. Otwinowski[85] , K. Oyama[82] , K. Ozawa[113] , Y. Pachmayer[82] , M. Pachr[33] , F. Padilla[22] , P. Pagano[25] , G. Paić[55] , F. Painke[35] , C. Pajares[12] , S.K. Pal[116] , A. Palaha[90] , A. Palmeri[99] , V. Papikyan[121] , G.S. Pappalardo[99] , W.J. Park[85] , A. Passfeld[54] , B. Pastirčák[47] , D.I. Patalakha[43] , V. Paticchio[98] , A. Pavlinov[119] , T. Pawlak[118] , T. Peitzmann[45] , H. Pereira Da Costa[11] , E. Pereira De Oliveira Filho[107] , D. Peresunko[88] , C.E. Pérez Lara[72] , E. Perez Lezama[55] , D. Perini[29] , D. Perrino[27] , W. Peryt[118] , A. Pesci[97] , V. Peskov[29 ,55] , Y. Pestov[3] , V. Petráček[33] , M. Petran[33] , M. Petris[70] , P. Petrov[90] , M. Petrovici[70] , C. Petta[24] , S. Piano[92] , A. Piccotti[94] , M. Pikna[32] , P. Pillot[102] , O. Pinazza[29] , L. Pinsky[110] , N. Pitz[52] , D.B. Piyarathna[110] , M. Płoskoń[67] , J. Pluta[118] , T. Pocheptsov[59] , S. Pochybova[60] , P.L.M. Podesta-Lerma[106] , M.G. Poghosyan[29 ,22] , K. Polák[49] , B. Polichtchouk[43] , A. Pop[70] , S. Porteboeuf-Houssais[63] , V. Pospíšil[33] , B. Potukuchi[80] , S.K. Prasad[119] , R. Preghenella[97 ,9] , F. Prino[94] , C.A. Pruneau[119] , I. Pshenichnov[44] , S. Puchagin[87] , G. Puddu[21] , A. Pulvirenti[24] , V. Punin[87] , M. Putiš[34] , J. Putschke[119 ,120] , E. Quercigh[29] , H. Qvigstad[17] , A. Rachevski[92] , A. Rademakers[29] , T.S. Räihä[37] , J. Rak[37] , A. Rakotozafindrabe[11] , L. Ramello[26] , A. Ramírez Reyes[8] , R. Raniwala[81] , S. Raniwala[81] , S.S. Räsänen[37] , B.T. Rascanu[52] , D. Rathee[77] , K.F. Read[112] , J.S. Real[64] , K. Redlich[100 ,57] , P. Reichelt[52] , M. Reicher[45] , R. Renfordt[52] , A.R. Reolon[65] , A. Reshetin[44] , F. Rettig[35] , J.-P. Revol[29] , K. Reygers[82] , L. Riccati[94] , R.A. Ricci[66] , T. Richert[28] , M. Richter[17] , P. Riedler[29] , W. Riegler[29] , F. Riggi[24 ,99] , B. Rodrigues Fernandes Rabacal[29] , M. Rodríguez Cahuantzi[1] , A. Rodriguez Manso[72] , K. Røed[14] , D. Rohr[35] , D. Röhrich[14] , R. Romita[85] , F. Ronchetti[65] , P. Rosnet[63] , S. Rossegger[29] , A. Rossi[29 ,19] ,

C. Roy[58] , P. Roy[89] , A.J. Rubio Montero[7] , R. Rui[20] , R. Russo[22] , E. Ryabinkin[88] , A. Rybicki[104] , S. Sadovsky[43] , K. Šafařík[29] , R. Sahoo[41] , P.K. Sahu[48] , J. Saini[116] , H. Sakaguchi[38] , S. Sakai[67] , D. Sakata[114] , C.A. Salgado[12] , J. Salzwedel[15] , S. Sambyal[80] , V. Samsonov[75] , X. Sanchez Castro[58] , L. Šándor[47] , A. Sandoval[56] , M. Sano[114] , S. Sano[113] , R. Santo[54] , R. Santoro[98 ,29 ,9] , J. Sarkamo[37] , E. Scapparone[97] , F. Scarlassara[19] , R.P. Scharenberg[83] , C. Schiaua[70] , R. Schicker[82] , C. Schmidt[85] , H.R. Schmidt[115] , S. Schreiner[29] , S. Schuchmann[52] , J. Schukraft[29] , Y. Schutz[29 ,102] , K. Schwarz[85] , K. Schweda[85 ,82] , G. Scioli[18] , E. Scomparin[94] , R. Scott[112] , P.A. Scott[90] , G. Segato[19] , I. Selyuzhenkov[85] , S. Senyukov[26 ,58] , J. Seo[84] , S. Serci[21] , E. Serradilla[7 ,56] , A. Sevcenco[50] , A. Shabetai[102] , G. Shabratova[59] , R. Shahoyan[29] , S. Sharma[80] , N. Sharma[77] , S. Rohni[80] , K. Shigaki[38] , M. Shimomura[114] , K. Shtejer[6] , Y. Sibiriak[88] , M. Siciliano[22] , E. Sicking[29] , S. Siddhanta[96] , T. Siemiarczuk[100] , D. Silvermyr[74] , C. Silvestre[64] , G. Simatovic[55 ,86] , G. Simonetti[29] , R. Singaraju[116] , R. Singh[80] , S. Singha[116] , V. Singhal[116] , T. Sinha[89] , B.C. Sinha[116] , B. Sitar[32] , M. Sitta[26] , T.B. Skaali[17] , K. Skjerdal[14] , R. Smakal[33] , N. Smirnov[120] , R.J.M. Snellings[45] , C. Søgaard[71] , R. Soltz[68] , H. Son[16] , J. Song[84] , M. Song[123] , C. Soos[29] , F. Soramel[19] , I. Sputowska[104] , M. Spyropoulou-Stassinaki[78] , B.K. Srivastava[83] , J. Stachel[82] , I. Stan[50] , I. Stan[50] , G. Stefanek[100] , M. Steinpreis[15] , E. Stenlund[28] , G. Steyn[79] , J.H. Stiller[82] , D. Stocco[102] , M. Stolpovskiy[43] , K. Strabykin[87] , P. Strmen[32] , A.A.P. Suaide[107] , M.A. Subieta Vásquez[22] , T. Sugitate[38] , C. Suire[42] , M. Sukhorukov[87] , R. Sultanov[46] , M. Šumbera[73] , T. Susa[86] , A. Szanto de Toledo[107] , I. Szarka[32] , A. Szczepankiewicz[104 ,29] , A. Szostak[14] , M. Szymański[118] , J. Takahashi[108] , J.D. Tapia Takaki[42] , A. Tauro[29] , G. Tejeda Muñoz[1] , A. Telesca[29] , C. Terrevoli[27] , J. Thäder[85] , D. Thomas[45] , R. Tieulent[109] , A.R. Timmins[110] , D. Tlusty[33] , A. Toia[35 ,19] , H. Torii[113] , L. Toscano[94] , V. Trubnikov[2] , D. Truesdale[15] , W.H. Trzaska[37] , T. Tsuji[113] , A. Tumkin[87] , R. Turrisi[93] , T.S. Tveter[17] , J. Ulery[52] , K. Ullaland[14] , J. Ulrich[61 ,51] , A. Uras[109] , J. Urbán[34] , G.M. Urciuoli[95] , G.L. Usai[21] , M. Vajzer[33 ,73] , M. Vala[59 ,47] , L. Valencia Palomo[42] , S. Vallero[82] , N. van der Kolk[72] , P. Vande Vyvre[29] , M. van Leeuwen[45] , L. Vannucci[66] , A. Vargas[1] , R. Varma[40] , M. Vasileiou[78] , A. Vasiliev[88] , V. Vechernin[117] , M. Veldhoen[45] , M. Venaruzzo[20] , E. Vercellin[22] , S. Vergara[1] , R. Vernet[5] , M. Verweij[45] , L. Vickovic[103] , G. Viesti[19] , O. Vikhlyantsev[87] , Z. Vilakazi[79] , O. Villalobos Baillie[90] , A. Vinogradov[88] , L. Vinogradov[117] , Y. Vinogradov[87] , T. Virgili[25] , Y.P. Viyogi[116] , A. Vodopyanov[59] , K. Voloshin[46] , S. Voloshin[119] , G. Volpe[27 ,29] , B. von Haller[29] , D. Vranic[85] , G. Øvrebekk[14] , J. Vrláková[34] , B. Vulpescu[63] , A. Vyushin[87] , B. Wagner[14] , V. Wagner[33] , R. Wan[39] , M. Wang[39] , D. Wang[39] , Y. Wang[82] , Y. Wang[39] , K. Watanabe[114] , M. Weber[110] , J.P. Wessels[29 ,54] , U. Westerhoff[54] , J. Wiechula[115] , J. Wikne[17] , M. Wilde[54] , A. Wilk[54] , G. Wilk[100] , M.C.S. Williams[97] , B. Windelband[82] , L. Xaplanteris Karampatsos[105] , C.G. Yaldo[119] , Y. Yamaguchi[113] , H. Yang[11] , S. Yang[14] , S. Yasnopolskiy[88] , J. Yi[84] , Z. Yin[39] , I.-K. Yoo[84] , J. Yoon[123] , W. Yu[52] , X. Yuan[39] , I. Yushmanov[88] , C. Zach[33] , C. Zampolli[97] , S. Zaporozhets[59] , A. Zarochentsev[117] , P. Závada[49] , N. Zaviyalov[87] , H. Zbroszczyk[118] , P. Zelnicek[51] , I.S. Zgura[50] , M. Zhalov[75] , H. Zhang[39] , X. Zhang[63 ,39] , F. Zhou[39] , Y. Zhou[45] , D. Zhou[39] , X. Zhu[39] , J. Zhu[39] , J. Zhu[39] , A. Zichichi[18 ,9] , A. Zimmermann[82] , G. Zinovjev[2] , Y. Zoccarato[109] , M. Zynovyev[2] , M. Zyzak[52]

Affiliation notes

[i] Also at: M.V.Lomonosov Moscow State University, D.V.Skobeltsyn Institute of Nuclear Physics, Moscow, Russia

[ii] Also at: University of Belgrade, Faculty of Physics and ”Vinča” Institute of Nuclear Sciences, Belgrade, Serbia

Collaboration Institutes

[1] Benemérita Universidad Autónoma de Puebla, Puebla, Mexico

[2] Bogolyubov Institute for Theoretical Physics, Kiev, Ukraine

[3] Budker Institute for Nuclear Physics, Novosibirsk, Russia

[4] California Polytechnic State University, San Luis Obispo, California, United States

[5] Centre de Calcul de l’IN2P3, Villeurbanne, France

[6] Centro de Aplicaciones Tecnológicas y Desarrollo Nuclear (CEADEN), Havana, Cuba

[7] Centro de Investigaciones Energéticas Medioambientales y Tecnológicas (CIEMAT), Madrid, Spain

[8] Centro de Investigación y de Estudios Avanzados (CINVESTAV), Mexico City and Mérida, Mexico

[9] Centro Fermi – Centro Studi e Ricerche e Museo Storico della Fisica “Enrico Fermi”, Rome, Italy

[10] Chicago State University, Chicago, United States

[11] Commissariat à l’Energie Atomique, IRFU, Saclay, France

[12] Departamento de Física de Partículas and IGFAE, Universidad de Santiago de Compostela, Santiago de Compostela, Spain
[13] Department of Physics Aligarh Muslim University, Aligarh, India
[14] Department of Physics and Technology, University of Bergen, Bergen, Norway
[15] Department of Physics, Ohio State University, Columbus, Ohio, United States
[16] Department of Physics, Sejong University, Seoul, South Korea
[17] Department of Physics, University of Oslo, Oslo, Norway
[18] Dipartimento di Fisica dell'Università and Sezione INFN, Bologna, Italy
[19] Dipartimento di Fisica dell'Università and Sezione INFN, Padova, Italy
[20] Dipartimento di Fisica dell'Università and Sezione INFN, Trieste, Italy
[21] Dipartimento di Fisica dell'Università and Sezione INFN, Cagliari, Italy
[22] Dipartimento di Fisica dell'Università and Sezione INFN, Turin, Italy
[23] Dipartimento di Fisica dell'Università 'La Sapienza' and Sezione INFN, Rome, Italy
[24] Dipartimento di Fisica e Astronomia dell'Università and Sezione INFN, Catania, Italy
[25] Dipartimento di Fisica 'E.R. Caianiello' dell'Università and Gruppo Collegato INFN, Salerno, Italy
[26] Dipartimento di Scienze e Innovazione Tecnologica dell'Università del Piemonte Orientale and Gruppo Collegato INFN, Alessandria, Italy
[27] Dipartimento Interateneo di Fisica 'M. Merlin' and Sezione INFN, Bari, Italy
[28] Division of Experimental High Energy Physics, University of Lund, Lund, Sweden
[29] European Organization for Nuclear Research (CERN), Geneva, Switzerland
[30] Fachhochschule Köln, Köln, Germany
[31] Faculty of Engineering, Bergen University College, Bergen, Norway
[32] Faculty of Mathematics, Physics and Informatics, Comenius University, Bratislava, Slovakia
[33] Faculty of Nuclear Sciences and Physical Engineering, Czech Technical University in Prague, Prague, Czech Republic
[34] Faculty of Science, P.J. Šafárik University, Košice, Slovakia
[35] Frankfurt Institute for Advanced Studies, Johann Wolfgang Goethe-Universität Frankfurt, Frankfurt, Germany
[36] Gangneung-Wonju National University, Gangneung, South Korea
[37] Helsinki Institute of Physics (HIP) and University of Jyväskylä, Jyväskylä, Finland
[38] Hiroshima University, Hiroshima, Japan
[39] Hua-Zhong Normal University, Wuhan, China
[40] Indian Institute of Technology, Mumbai, India
[41] Indian Institute of Technology Indore (IIT), Indore, India
[42] Institut de Physique Nucléaire d'Orsay (IPNO), Université Paris-Sud, CNRS-IN2P3, Orsay, France
[43] Institute for High Energy Physics, Protvino, Russia
[44] Institute for Nuclear Research, Academy of Sciences, Moscow, Russia
[45] Nikhef, National Institute for Subatomic Physics and Institute for Subatomic Physics of Utrecht University, Utrecht, Netherlands
[46] Institute for Theoretical and Experimental Physics, Moscow, Russia
[47] Institute of Experimental Physics, Slovak Academy of Sciences, Košice, Slovakia
[48] Institute of Physics, Bhubaneswar, India
[49] Institute of Physics, Academy of Sciences of the Czech Republic, Prague, Czech Republic
[50] Institute of Space Sciences (ISS), Bucharest, Romania
[51] Institut für Informatik, Johann Wolfgang Goethe-Universität Frankfurt, Frankfurt, Germany
[52] Institut für Kernphysik, Johann Wolfgang Goethe-Universität Frankfurt, Frankfurt, Germany
[53] Institut für Kernphysik, Technische Universität Darmstadt, Darmstadt, Germany
[54] Institut für Kernphysik, Westfälische Wilhelms-Universität Münster, Münster, Germany
[55] Instituto de Ciencias Nucleares, Universidad Nacional Autónoma de México, Mexico City, Mexico
[56] Instituto de Física, Universidad Nacional Autónoma de México, Mexico City, Mexico
[57] Institut of Theoretical Physics, University of Wroclaw
[58] Institut Pluridisciplinaire Hubert Curien (IPHC), Université de Strasbourg, CNRS-IN2P3, Strasbourg, France
[59] Joint Institute for Nuclear Research (JINR), Dubna, Russia
[60] KFKI Research Institute for Particle and Nuclear Physics, Hungarian Academy of Sciences, Budapest, Hungary

[61] Kirchhoff-Institut für Physik, Ruprecht-Karls-Universität Heidelberg, Heidelberg, Germany
[62] Korea Institute of Science and Technology Information, Daejeon, South Korea
[63] Laboratoire de Physique Corpusculaire (LPC), Clermont Université, Université Blaise Pascal, CNRS–IN2P3, Clermont-Ferrand, France
[64] Laboratoire de Physique Subatomique et de Cosmologie (LPSC), Université Joseph Fourier, CNRS-IN2P3, Institut Polytechnique de Grenoble, Grenoble, France
[65] Laboratori Nazionali di Frascati, INFN, Frascati, Italy
[66] Laboratori Nazionali di Legnaro, INFN, Legnaro, Italy
[67] Lawrence Berkeley National Laboratory, Berkeley, California, United States
[68] Lawrence Livermore National Laboratory, Livermore, California, United States
[69] Moscow Engineering Physics Institute, Moscow, Russia
[70] National Institute for Physics and Nuclear Engineering, Bucharest, Romania
[71] Niels Bohr Institute, University of Copenhagen, Copenhagen, Denmark
[72] Nikhef, National Institute for Subatomic Physics, Amsterdam, Netherlands
[73] Nuclear Physics Institute, Academy of Sciences of the Czech Republic, Řež u Prahy, Czech Republic
[74] Oak Ridge National Laboratory, Oak Ridge, Tennessee, United States
[75] Petersburg Nuclear Physics Institute, Gatchina, Russia
[76] Physics Department, Creighton University, Omaha, Nebraska, United States
[77] Physics Department, Panjab University, Chandigarh, India
[78] Physics Department, University of Athens, Athens, Greece
[79] Physics Department, University of Cape Town, iThemba LABS, Cape Town, South Africa
[80] Physics Department, University of Jammu, Jammu, India
[81] Physics Department, University of Rajasthan, Jaipur, India
[82] Physikalisches Institut, Ruprecht-Karls-Universität Heidelberg, Heidelberg, Germany
[83] Purdue University, West Lafayette, Indiana, United States
[84] Pusan National University, Pusan, South Korea
[85] Research Division and ExtreMe Matter Institute EMMI, GSI Helmholtzzentrum für Schwerionenforschung, Darmstadt, Germany
[86] Rudjer Bošković Institute, Zagreb, Croatia
[87] Russian Federal Nuclear Center (VNIIEF), Sarov, Russia
[88] Russian Research Centre Kurchatov Institute, Moscow, Russia
[89] Saha Institute of Nuclear Physics, Kolkata, India
[90] School of Physics and Astronomy, University of Birmingham, Birmingham, United Kingdom
[91] Sección Física, Departamento de Ciencias, Pontificia Universidad Católica del Perú, Lima, Peru
[92] Sezione INFN, Trieste, Italy
[93] Sezione INFN, Padova, Italy
[94] Sezione INFN, Turin, Italy
[95] Sezione INFN, Rome, Italy
[96] Sezione INFN, Cagliari, Italy
[97] Sezione INFN, Bologna, Italy
[98] Sezione INFN, Bari, Italy
[99] Sezione INFN, Catania, Italy
[100] Soltan Institute for Nuclear Studies, Warsaw, Poland
[101] Nuclear Physics Group, STFC Daresbury Laboratory, Daresbury, United Kingdom
[102] SUBATECH, Ecole des Mines de Nantes, Université de Nantes, CNRS-IN2P3, Nantes, France
[103] Technical University of Split FESB, Split, Croatia
[104] The Henryk Niewodniczanski Institute of Nuclear Physics, Polish Academy of Sciences, Cracow, Poland
[105] The University of Texas at Austin, Physics Department, Austin, TX, United States
[106] Universidad Autónoma de Sinaloa, Culiacán, Mexico
[107] Universidade de São Paulo (USP), São Paulo, Brazil
[108] Universidade Estadual de Campinas (UNICAMP), Campinas, Brazil
[109] Université de Lyon, Université Lyon 1, CNRS/IN2P3, IPN-Lyon, Villeurbanne, France
[110] University of Houston, Houston, Texas, United States
[111] University of Technology and Austrian Academy of Sciences, Vienna, Austria
[112] University of Tennessee, Knoxville, Tennessee, United States
[113] University of Tokyo, Tokyo, Japan

[114] University of Tsukuba, Tsukuba, Japan
[115] Eberhard Karls Universität Tübingen, Tübingen, Germany
[116] Variable Energy Cyclotron Centre, Kolkata, India
[117] V. Fock Institute for Physics, St. Petersburg State University, St. Petersburg, Russia
[118] Warsaw University of Technology, Warsaw, Poland
[119] Wayne State University, Detroit, Michigan, United States
[120] Yale University, New Haven, Connecticut, United States
[121] Yerevan Physics Institute, Yerevan, Armenia
[122] Yildiz Technical University, Istanbul, Turkey
[123] Yonsei University, Seoul, South Korea
[124] Zentrum für Technologietransfer und Telekommunikation (ZTT), Fachhochschule Worms, Worms, Germany